

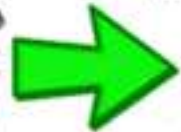
Model substrate



Real substrate



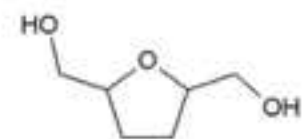
Hydrolyzate from fructose



BHMF yield up to 93 mol%



Polyesters



BHMTHF yield up to 95 mol%



Polyurethanes

Highlights

- The tunable hydrogenation of both aqueous HMF solutions and crude fructose hydrolyzate to renewable diols BHMF and BHMTHF, was studied.
- 5 wt% Ru/C resulted an active and robust catalyst, showing negligible sintering and leaching processes.
- Yields of BHMF up to 93 mol% and of BHMTHF up to 95 mol% were ascertained starting from aqueous HMF.
- This study proves the feasibility of renewable monomers synthesis from the crude fructose hydrolyzate, opening the way for their production directly from lignocellulosic biomass through a cascade process.

1 **Insight into the hydrogenation of pure and crude HMF to furan diols**
2 **using Ru/C as catalyst**

3 Sara Fulignati^a, Claudia Antonetti^a, Domenico Licursi^a, Matteo Pieraccioni^a, Erwin
4 Wilbers^b, Hero Jan Heeres^b, Anna Maria Raspolli Galletti^{a,*}

5
6 ^aDepartment of Chemistry and Industrial Chemistry, University of Pisa, Via G. Moruzzi
7 13, 56124, Pisa, Italy

8 ^bGreen Chemical Reaction Engineering, ENTEG, University of Groningen, Nijenborgh
9 4, 9747 AG Groningen, The Netherlands

10

11 **Abstract**

12 5-hydroxymethylfurfural (HMF) is one of the most important renewable platform-
13 chemicals, a very valuable precursor for the synthesis of bio-fuels and bio-products. In
14 this work, the hydrogenation of HMF to two furan diols, 2,5-bis(hydroxymethyl)furan
15 (BHMF) and 2,5-bis(hydroxymethyl)tetrahydrofuran (BHMTHF), both promising
16 renewable monomers, was investigated. Three commercial catalysts, Ru/C, Pd/C and
17 Pt/C, were tested in the hydrogenation of aqueous HMF solutions (2-3 wt%), using a
18 metal loading of 1 wt% respect to HMF content. By appropriate tuning of the process
19 conditions, either BHMF or BHMTHF were obtained in good yields, and Ru/C resulted
20 the best catalyst for this purpose, allowing us to obtain BHMF or BHMTHF yields up to
21 93.0 and 95.3 mol%, respectively. This catalyst was also tested for in the hydrogenation
22 of a crude HMF-rich hydrolyzate, obtained by one-pot the dehydration of fructose. The
23 influence of each component of this hydrolyzate on the hydrogenation efficiency was
24 investigated, including unconverted fructose, rehydration acids and humins, in order to
25 improve the yields towards each furan diol. Moreover, ICP-OES and TEM analysis

26 showed that the catalyst was not subjected to **important** leaching and sintering
27 phenomena, as **further** confirmed by catalyst recycling **study**.

28

29 **Keywords**

30 5-hydroxymethylfurfural; aqueous-phase hydrogenation; 2,5-bis(hydroxymethyl)furan;
31 2,5-bis(hydroxymethyl)tetrahydrofuran; crude hydrolyzate.

32

33 *Corresponding author, e-mail: anna.maria.raspolli.galletti@unipi.it

34

35 **1. Introduction**

36 Nowadays, the dwindling supplies of worldwide fossil resources and the growth of
37 carbon dioxide emission make the production of chemicals and fuels from renewable
38 resources a key topic of the industrial chemistry [1-3]. Biomass is a very promising
39 alternative feedstock, being abundant, cheap, widespread and precursor for **the**
40 **production of** several valuable products [4-6]. In particular, 5-hydroxymethylfurfural
41 (HMF) is considered as one of the most important bio-based compounds [7]. HMF may
42 be obtained by the dehydration of **model compounds, including** monosaccharides, such
43 as glucose [8-11] and fructose [11-15], polysaccharides, such as inulin [12,13,16],
44 starch [11,15] and cellulose [11,15,17,18] and, **more advantageously, real**
45 lignocellulosic biomasses, such as corn stover, pinewood, switchgrass and poplar
46 [14,19]. The presence of different reactive groups (an **aldehyde** group, a hydroxyl group
47 and a furan ring) makes HMF a very important platform-chemical, precursor of bio-
48 fuels, such as 2,5-dimethylfuran (DMF) [20,21], 5-ethoxymethylfurfural (EMF) [22]
49 and long chain alkanes [23]. In addition, it is possible to convert HMF into interesting
50 monomers, such as 2,5-furandicarboxylic acid (FDCA) [24,25], 2,5-

51 bis(hydroxymethyl)furan (BHMF) [26-28], 2,5-bis(hydroxymethyl)tetrahydrofuran
52 (BHMTHF) [29-31] and caprolactone [32] and many more valuable products [33-35].
53 In this work, the selective synthesis of two important furan diols, BHMF and
54 BHMTHF, is investigated. The first one derives from the hydrogenation of the aldehyde
55 group of HMF, whereas the second one stems from the hydrogenation of both aldehyde
56 group and furan ring. Their application for the synthesis of resins, fibres, foams and
57 polymers has been recently proven, underlining their high potential as monomers for the
58 synthesis of alternative and renewable materials [36-40]. Regarding their possible
59 synthesis, the majority of the literature investigations employs molecular hydrogen as
60 reducing agent, in particular for the synthesis of BHMTHF, whereas the hydrogenation
61 of HMF to BHMF has been also carried out using formic acid [41] or isopropanol
62 [42,43] as hydrogen donor, or through electrochemical processes [28]. Concerning the
63 catalyst selection, mainly heterogeneous catalysts have been used and only a few papers
64 have described the use of homogeneous ones [41, 44]. Advantages of the former are
65 ease of separation from the reaction medium and recyclability. The most largely
66 adopted heterogeneous catalysts are represented by metals, such as Ru, Pt, Pd, Au, Ir,
67 Ni, Cu supported on several oxides, polymers or carbon species [3,30,36,45-53]. Ru-,
68 Pd-, and Pt-catalysts are particularly attractive for this purpose, because of their high
69 intrinsic activity, and it is usually easy to have them dispersed as nanoparticles on an
70 appropriate support [53]. In most of the published works, the HMF hydrogenation has
71 been carried out working with toxic, expensive, and non-renewable solvents, such as
72 ionic liquids and organic solvents (mainly tetrahydrofuran, 1,4-dioxane and alcohols).
73 However, from a green chemistry point of view, the use of water is certainly preferred.
74 In addition, the HMF upgrading in water is of more practical importance, because HMF
75 is expected to be directly supplied as an aqueous solution in a biorefinery process, thus
76 minimizing or, even better, avoiding expensive and unnecessary purification steps.

77 Unfortunately, lower diols selectivities are reported when the reaction is performed in
78 water, rather than in organic or biphasic solvent systems [30,54,55]. In fact, water-based
79 HMF hydrogenation may lead to different products, because this reaction environment
80 could enable the hydrolytic ring opening, the hydrodeoxygenation and rearrangements
81 of the furan ring. On this basis, the selectivity of the water-based hydrogenation of
82 HMF to BHMF and BHMTHF is markedly determined by the hydrogenation activity
83 and acid–base properties of the chosen catalytic system. Functional sites determine the
84 selectivity of products in a catalytic reaction system for the hydrogenation of HMF in
85 water, using supported metal catalysts, in particular the metal surface for
86 hydrogenation/hydrogenolysis, the support surface for acid–base catalysis, the metal-
87 support interface for the unique adsorption of reactants, and the acid–base catalysis,
88 determined by the presence of water and other compounds of the reaction mixture.
89 Focusing the attention on the catalysts of interest in this work, the best results in
90 aqueous medium have been obtained using non-commercial, *ad hoc* synthesized
91 catalysts. In this regard, Chen et al. [46] carried out the hydrogenation of diluted
92 aqueous HMF solution employing Ru clusters immobilized on nanosized mesoporous
93 zirconium silica (Ru/MSN-Zr) as catalyst, reaching the maximum BHMF yield of 90
94 mol%. They have also investigated the synthesis of BHMTHF from HMF in water [48]
95 adopting Pd catalyst supported on amine-functionalized metal-organic frameworks
96 (Pd/MIL-101(Al)-NH₂), obtaining the BHMTHF yield of 96 mol%. Despite the
97 promising catalytic performances of many *ad hoc* synthesised catalysts, some problems
98 still limit their application on a larger scale, such as the reproducibility of catalyst
99 formulation (and therefore of its properties), the cost of recovery of the precious metal
100 from the spent catalyst after its use, the cost of the support and catalyst production.
101 Commercial catalysts still remain the preferred choice for hydrogenation reactions, in
102 particular those carbon-based, because of their lower cost, high surface area, chemical

103 inertness, thermal stability in non-oxidizing atmospheres, and ease of metal recovery,
104 allowed by simple calcination. The use of commercial catalysts for the synthesis of the
105 diols was reported by Schiavo et al. [57]. A wide range of noble metals supported on
106 carbon, such as 10 wt% Pd/C, 10 wt% Pt/C and 10 wt% Ru/C, was tested together with
107 Raney Ni, platinum oxide and copper chromite. All catalysts were active towards the
108 HMF hydrogenation in water to BHMF and BHMTHF and, particularly, 10 wt% Ru/C
109 showed promising results, by properly tuning the reaction time. In particular, the BHMF
110 yield of 95 mol% was obtained after 30 min, whereas prolonging the reaction to 4 h
111 gave the BHMTHF yield of 92 mol%. These results were obtained adopting a low HMF
112 concentration (1.3 wt%), which could be responsible of the ascertained good selectivity.
113 Moreover, the authors did not perform a systematic investigation and they did not study
114 the influence of the main reaction parameters to give the target diols. Regarding the
115 possible role of the catalytic support, Alamillo et al. [30] proved that acidic supports,
116 such as SiO₂, have a detrimental role on the HMF hydrogenation, favouring the
117 selective formation of ring opening triols and tetrol, such as 1,2,5-hexanetriol, 1,2,5,6-
118 hexanetetrol and 1,2,6-hexanetirol, formed by the hydrogenation of acid-catalyzed
119 degradation products of BHMF. In this context, also the presence of other homogeneous
120 acids, which are typical of the hydrolyzate solutions, such as H₂SO₄ and levulinic acid,
121 also caused a significant reduction of furan diols selectivity. These statements suggest
122 that the pH of the aqueous reaction solution has certainly a strong influence on the furan
123 diols selectivity and, in particular, a low pH causes undesired ring opening and also
124 degradation of HMF and reaction intermediates, leading to the undesired formation of
125 humins. This issue could be partially solved on laboratory scale by using a biphasic
126 system, which allows HMF extraction from the aqueous phase, minimizing its
127 degradation to acids and humins. This application is still academically interesting, even
128 if not very practical from an industrial point of view. In this context, Alamillo et al. [30]

129 studied the activity of Ru black in different solvents and the highest BHMTFH
130 selectivity (67 mol%) at complete HMF conversion was obtained using
131 tetrahydrofurfuryl alcohol, whereas it markedly decreased to 46 mol% employing the
132 biphasic water/1-butanol (1/2 v/v) system and even more in water (22 mol%). The
133 decrease of BHMTFH yield was attributed to the formation of polyols, such as 1,2,6-
134 hexanetriol and 1,2,5-hexanetriol, deriving from the hydration of the intermediate
135 BHMF, together with additional degradation pathways occurring in water. In addition to
136 the acid–base properties of a reaction system, also the hydrogenation rate has an
137 influence on the yield or selectivity of BHMF and BHMTFH, because BHMF is
138 relatively unstable under hydrothermal reaction conditions. In this sense, the maximum
139 yield of BHMF can be obtained by increasing the hydrogenation rate of HMF beyond
140 that of BHMF ring opening. On the basis of the above statements, HMF hydrogenation
141 in water is certainly challenging for industrial applications, but very difficult to tune,
142 depending on the contribute of many different components, which simultaneously act
143 within the reaction environment, and which must be individually and experimentally
144 considered, for a better understanding of the reaction.

145 Starting from the work of Schiavo et al. [30], in this work, the hydrogenation of more
146 concentrated HMF aqueous solution (2-3 wt%) has been carried out in the presence of
147 commercial noble metals supported on carbon, Ru/C, Pd/C and Pt/C. The choice of
148 carbon support for this purpose is appropriate, thanks to its relative inertness, which
149 prevents the occurrence of unwanted reactions catalyzed by the support surface acidity,
150 thus allowing us to focus the attention on the sole effect of the reaction mixture. The
151 adopted HMF concentration was similar to that reached in water for crude HMF
152 synthesis from fructose hydrolysis, previously optimized by us [13]. The BHMF and
153 BHMTFH yields have been optimized by properly tuning the process conditions, in
154 order to minimize the ring opening issue. These optimized reaction conditions have

155 been **subsequently** employed in the cascade process for the direct hydrogenation of the
156 HMF-rich crude hydrolyzate obtained from the dehydration of fructose to HMF,
157 without any intermediate separation step. With this approach, the intermediate
158 separation and purification steps to obtain pure HMF are avoided, **because unnecessary**,
159 with a positive impact on the techno-economic viability of the overall process from
160 fructose to renewable **furan** diols.

161

162 **2. Methods**

163 *2.1 Materials*

164 5-hydroxymethylfurfural (95%) was supplied by AVA Biochem. 2,5-
165 bis(hydroxymethyl)furan (95%) and 2,5-bis(hydroxymethyl)tetrahydrofuran (95%)
166 were provided by AKos GmbH (Germany). Ru/C (5 wt%), Pd/C (5 wt%), formic acid
167 (99.8%), levulinic acid (98%), ethanol (**96%**), dichloromethane (99.9%), sodium
168 bicarbonate and water for HPLC were purchased from Sigma-Aldrich. Pt/C (5 wt%)
169 was supplied by Strem Chemicals. Fructose was food grade. Amberlyst-70 was
170 provided by Rohm and Haas. All catalysts and chemicals were employed as received.

171 *2.2 Hydrogenation of HMF*

172 Hydrogenation reactions were carried out in a 300 mL stainless steel Parr 4560
173 autoclave equipped with a P.I.D. controller (4843). In **a typical** experiment, a weight
174 ratio metal to HMF of 1 wt% was used. **In this regard, the catalyst employed as**
175 **received, was weighted and introduced into the autoclave, which was subsequently**
176 **closed and evacuated to 65 Pa with a mechanical vacuum pump. 50 mL of a HMF**
177 **aqueous solution was introduced into the autoclave by suction, and the reaction mixture**
178 **was stirred using a mechanical overhead stirrer. Then,** the reactor was pressurized with
179 hydrogen till the desired pressure was reached at the pre-set temperature, **always under**
180 mechanical stirring. The pressure in the reactor was manually held constant at the pre-

181 determined value by repeated hydrogen addition, **when necessary**. The reaction progress
182 was monitored by sampling periodically the liquid through a dip tube. The liquid
183 samples were analysed using HPLC. All the experiments were carried out in triplicate
184 and the reproducibility of the techniques was within 3%. For the **recycling** tests, the
185 employed catalyst was recovered by filtration and **re-used within** two subsequent runs.
186 At the end of the third cycle, the recovered catalyst was washed with acetone, dried and
187 **re-used for an additional recycling** test.

188 *2.3 Synthesis of a HMF-rich hydrolyzate from fructose*

189 The hydrolyzate was prepared using a microwave reactor CEM Discover S-class
190 System, according to the procedure reported by Antonetti et al. at optimum reaction
191 conditions [13]. At the end of the **hydrolysis** reaction, the heterogeneous catalyst
192 Amberlyst-70 was separated **by the liquid fraction through** centrifugation, and the
193 isolated liquid fraction was employed as raw feedstock of the **subsequent**
194 hydrogenation.

195 *2.4 Hydrogenation of hydrolyzate with Ru/C*

196 **The hydrogenation of the HMF-rich hydrolyzate from fructose was conducted**
197 **analogously to that of pure HMF and, also in this case, a weight ratio metal to HMF of 1**
198 **wt% was adopted**. The **progress** of the reaction was monitored by sampling periodically
199 the liquid through a dip tube. The liquid samples were analyzed by HPLC.

200 *2.5 Analytical equipment*

201 *2.5.1 High-Pressure Liquid Chromatography*

202 High-pressure liquid chromatography (HPLC) analysis of the liquid samples deriving
203 from HMF hydrogenation runs was carried out with Perkin Elmer Flexer Isocratic
204 Platform equipped with a column Benson 2000-0 BP-OA (300 mm x 7.8 mm). A 0.005
205 M H₂SO₄ aqueous solution was adopted as mobile phase, maintaining the column at 60
206 °C with a flow-rate of 0.6 **mL/min**. The concentrations of products were determined

207 from calibration curves obtained with standard solutions. Conversion, products yield
208 and products selectivity were expressed in mol%. The carbon balance was evaluated as
209 the sum of the moles of products and unconverted HMF respect to the initial moles of
210 HMF and it was expressed in mol%.

211 *2.5.2 Gas Chromatography coupled with Mass Spectrometer*

212 The by-products formed during the hydrogenation of HMF were **qualitatively** identified
213 by gas chromatography coupled with mass spectrometer (GC-MS). Before the analysis,
214 the aqueous solution was extracted with dichlorometane. A GC-MS (Agilent 7890B-
215 5977A) equipped with HP-5MS capillary column (30 m × 0.25 mm × 0.25 μm) (5%-
216 phenyl)-methylpolysiloxane was employed for the analysis. The carrier gas was helium
217 with a flow of 1 mL/min. The injector and detector temperatures were **250 °C** and **280**
218 **°C**, respectively. The following temperature program was adopted for the
219 chromatographic run: 70 °C isothermal for 2 min; **12 °C/min** up to 250 °C; 250 °C
220 isothermal for 2 min.

221 *2.5.3 Transmission Electron Microscopy*

222 Transmission Electron Microscopy (TEM) measurements in bright field mode were
223 conducted with a CM12 microscope (Philips), operating at 120 keV. The catalysts were
224 suspended **in ethanol by ultra-sonication**, and the obtained sample was dropped onto
225 carbon coated 400 mesh copper grids. Images were taken on a slow scanning CCD
226 camera. The ruthenium particle size distribution was evaluated by measuring at least
227 100 particles with the software Nano Measurer 1.2.

228 *2.5.4 Nitrogen physisorption*

229 Nitrogen physisorption experiments were carried out in a Micromeritics ASAP 2020 at
230 -196.2 °C. Before the measurement, the samples were degassed under vacuum at 150
231 °C for 6 h. The surface area was estimated using the standard BET method. The single

232 point desorption total pore volume (VT) was calculated from the amount of gas
233 adsorbed at a relative pressure of 0.98 in the desorption branch.

234 *2.5.5 Thermogravimetric analysis*

235 Thermogravimetric analysis (TGA) of the fresh and used catalysts was determined
236 using a TGA Q50 system (TA Instrument). The samples were heated in a nitrogen
237 atmosphere, employing a temperature range between 20 and 650 °C, and a heating rate
238 of 10 °C/min.

239 *2.5.6 Inductively coupled plasma-optical emission spectrometry*

240 Inductively coupled plasma-optical emission spectrometry (ICP-OES) was employed to
241 determine the metal content in the catalyst after reaction using an Optima 7000 DV
242 (PerkinElmer) analyser equipped with a CCD array detector. **Sample digestion was**
243 **carried out in a microwave oven (CEM MARS 5). 20 mg of catalyst was weighted and**
244 **introduced in the vessel together with a mixture of HNO₃ (7 mL), HCl (1 mL) and HF**
245 **(2 mL). The vessel was closed and heated at 200 °C for 2 h. Subsequently, the vessel**
246 **was cooled to room temperature and diluted to 50 mL with double-distilled water, prior**
247 **to the ICP-OES analysis.**

248 *2.5.7 Gas-phase analysis*

249 **The Micro-GC Agilent 3000 equipped with a thermal conductivity detector was**
250 **employed for the CO identification. The channel used for CO analysis was the**
251 **molecular sieve column Molsieve 5A (10 m x 0.32 mm x 12 µm), adopting argon as**
252 **carrier gas.**

253 **3. Results and discussion**

254 *3.1 Metal species screening*

255 **Starting from the work of Schiavo et al. [30], a preliminary screening of the catalytic**
256 **performances of different commercial catalysts (Ru/C, Pd/C and Pt/C, 5 wt%) was**

257 performed at 140 °C, 70 bar H₂, with the initial HMF concentration of 2 wt% and the
258 metal to HMF ratio of 1 wt%. The results are reported in **Table 1**.

259 **Table 1**, near here

260 Pt/C resulted the least active system and the HMF conversion was only 64.5 mol% after
261 1 h of reaction. Both Pd/C and Ru/C were more active and complete HMF conversion
262 was reached after 1 h. Regarding products distribution, Pt/C gave a very low selectivity
263 to BHMF (< 16 mol%). GC-MS analysis of the reaction mixture (Figure S1) showed the
264 presence of several by-products **deriving** from the hydrodeoxygenation of HMF, such as
265 2,5-hexanedione, 5-methyl-2-furaldehyde and 5-hydroxy-2-hexanone (**Scheme 1A**), in
266 agreement with the literature [58].

267 **Scheme 1**, near here

268 **Under the adopted reaction conditions**, Pt/C mainly promotes the hydrodeoxygenation
269 and ring opening of HMF, resulting in a poor selectivity towards the desired **furan** diols.
270 On the other hand, **both** Pd/C and Ru/C favour hydrogenation reactions, leading to
271 improved BHMTHF yields (55.8 and 88.6 mol% for Pd/C and Ru/C, respectively).
272 **Among the three catalysts**, Ru/C is surely the most promising, combining high HMF
273 conversion with high BHMTHF selectivity, **as** also confirmed by the **best** carbon
274 balance, **the closest** to 90 mol%. In this case, only minor amounts of by-products were
275 detected, such as tetrahydrofurfuryl alcohol, 5-methyl-tetrahydrofurfuryl alcohol, 2,5-
276 dimethyltetrahydrofuran and tetrahydro-2H-pyran-2-methanol. These are known by-
277 products, **deriving** from BHMTHF degradation reactions which are promoted at
278 elevated temperatures [59] (Figure S2 and **Scheme 1B**). For Pd/C catalyst, not only the
279 hydrogenation of both aldehyde group and furan ring of HMF occurs, but also
280 hydrodeoxygenation and ring opening reactions (**Scheme 1C**), as ascertained by the
281 presence of typical by-products, such as 5-methyl-tetrahydrofurfuryl alcohol, 2,5-

282 hexanedione, 5-hydroxy-2-hexanone and 1,2,6-hexanetriol (Figure S3), in agreement
283 with the literature [55,60,61].

284 On the basis of this exploratory screening, Ru/C was identified as the most promising
285 commercial catalyst for the aqueous hydrogenation of HMF to the target diols, and
286 therefore it was adopted for subsequent optimization studies.

287 3.2 Optimization of BHMF and BHMTHF yields in the presence of Ru/C

288 The above reported preliminary screening has been performed under harsh reaction
289 conditions (140 °C and 70 bar H₂). Subsequently, in order to improve the selectivity of
290 the reaction, milder reaction conditions have been adopted, in terms of temperature and
291 H₂ pressure. In particular, the influence of temperature (100-140 °C) on the catalytic
292 performances at 70 bar H₂ was investigated, and the obtained results are reported in
293 Figure 1.

294 Figure 1, near here

295 The conversion of HMF was almost complete already at short reaction time (30 min),
296 for all the adopted temperatures. On the other hand, temperature strongly influenced the
297 products distribution. In fact, at 140 °C (Figure 1A), the amount of BHMF was
298 negligible during the whole reaction due to the extensive hydrogenation of the furan
299 ring and BHMTHF yield of 79.3 mol% was ascertained after 30 min. BHMTHF yield
300 reached the maximum value of 88.6 mol% after 60 min, and then decreased, due to the
301 formation of by-products, as evidenced by the corresponding trend of carbon balance
302 (run 4, Table S1). Working at 120 °C (Figure 1B), the hydrogenation of the furan ring
303 was slower and, after 30 min, the BHMF yield of 16.0 mol% was obtained. The
304 maximum BHMTHF yield shifted from 60 to 180 min (Figures 1A and 1B), when it
305 resulted higher than that ascertained at 140 °C, reaching 92.8 mol%. These results
306 underline that the by-products formation is favoured at high temperature, as confirmed
307 by the corresponding trend of carbon balance at the different temperatures reported in

308 **Table S1**, and by the results obtained decreasing the reaction temperature up to 100 °C
309 (Figure 1C). In fact, in this last case, the BHMTHF yield **continuously** increased **with**
310 **the** time, reaching the highest value of 95.0 mol% after 240 min.

311 On this basis, the effect of the decrease of H₂ pressure to 50 bar **was further investigated**
312 **working at 100 °C**, and the obtained results are reported in **Table 2**.

313 **Table 2**, near here

314 The decrease of H₂ pressure did not influence the HMF conversion, that resulted almost
315 complete (compare runs 7 and 8, **Table 2**) during the whole reaction. On the other hand,
316 at short reaction time (30 min), the lower pressure led to a higher BHMF yield at the
317 expense of BHMTHF yield, due to the reduced hydrogenation of the furan ring.

318 The concentration of the **starting** feedstock is another very important parameter because,
319 usually, high substrate concentrations promote side-reactions, and the yields and/or
320 selectivities towards target products fall down. The initial HMF concentration was
321 increased from 2 to 3 wt% (runs 8 and 9, **Table 2**) at 50 bar H₂, **on the basis of the HMF**
322 **concentration obtained from fructose in a previous study adopting Amberlyst A-70 as**
323 **acid catalyst in water [13], in the perspective of a feasible cascade approach.**

324 The presence of a higher amount of the initial substrate did not limit the hydrogenation
325 of the aldehyde group of HMF, whose conversion resulted unchanged, but caused a
326 slowdown of the furan ring hydrogenation, as **evidenced in particular** at short reaction
327 times. However, at the end of the reaction, analogous BHMTHF yields were ascertained
328 starting from 2 and 3 wt% HMF solutions. **Moreover, in order to prove the key role of**
329 **Ru/C towards the activation of the HMF hydrogenation, a blank run without the catalyst**
330 **was performed under the same reaction conditions (100 °C, 50 bar H₂, 3 wt% HMF**
331 **solution). In this case, after 240 min, the conversion of HMF resulted 10.6 mol% and**
332 **only BHMF in trace was detected, confirming the necessity of employing a suitable**
333 **catalyst for the hydrogenation of HMF. In conclusion, the highest BHMTHF yield of**

334 95.3 mol% was reached starting from 3 wt% HMF aqueous solution at 100 °C, 50 bar
335 H₂ after 240 min. This represents a very promising result, considering that BHMTHF
336 yields over 90 mol% have been reported working only on less concentrated water
337 solution, adopting higher H₂ pressures [56,57], and/or higher temperatures [57], longer
338 reaction times [48,57] and, in the presence of *ad hoc* synthesized catalysts, which are
339 not still really interesting for industrial applications in the immediate future.

340 Once having optimized the synthesis of BHMTHF, this study was focused on the
341 optimization of BHMF synthesis, where the sole hydrogenation of the aldehyde group
342 of HMF is required. The above results suggested that it was necessary to adopt milder
343 reaction conditions and thus, the H₂ pressure was reduced to 30 bar (run 10, Table 2).
344 The hydrogenation of HMF was slowed down and, for the first time, its conversion was
345 not complete within the first hour of reaction. As a consequence, also the hydrogenation
346 of the furan ring was limited, causing the increase of BHMF yield, which resulted 79.5
347 mol% after 30 min. However, under the H₂ pressure of 30 bar, BHMF underwent other
348 side-reactions, as evidenced by the worsening of the carbon balance in run 10, reaching
349 the value of 29.6 mol%, after 240 min. The pressure of 30 bar H₂ was not sufficient to
350 promote the hydrogenation of the furan ring, which requires high temperatures and high
351 pressures to occur [53]. However, as reported in the literature [59,62], at high
352 temperatures and low pressures, the ring opening of BHMF prevailed, resulting faster
353 than the hydrogenation of the furan ring. In fact, the low hydrogen pressure is
354 disadvantageous for hydrogen solubilisation in water, inhibiting the conversion of
355 BHMF to BHMTHF, and promoting the formation of partially hydrogenated products,
356 which are intermediates for the synthesis of polyols, such as 1,2,6-hexanetriol, 1,2-
357 hexanediol, 1,6-hexanediol, 1-hydroxyl-2,5-hexanedione and 1,2,5-hexanetriol [30, 59].
358 In fact, as reported in the literature, 1,2,6-hexanetriol derives from the ring opening of
359 BHMF and hydrogenation of the intermediate, whereas 1,2-hexanediol and 1,6-

360 hexanediol originate from the break of the C-O bond of C6 or C2 of 1,2,6-hexanetriol,
361 respectively [59]. Regarding 1-hydroxyl-2,5-hexanedione and 1,2,5-hexanetriol, the
362 first one derives from the rearrangement of BHMF, favoured in water, followed by ring
363 opening, whereas 1,2,5-hexanetriol is the product of 1-hydroxyl-2,5-hexanedione
364 complete hydrogenation [30]. In order to optimize the BHMF production, the
365 investigation of temperature within the range 50-120 °C was carried out at 30 bar H₂,
366 and the results are reported in Figure 2.

367  Figure 2, near here

368 As expected, HMF conversion increased with temperature, which strongly influences
369 the distribution of products. In fact, when the reaction was performed at 50 °C, the
370 BHMF yield continuously increased, reaching the highest value of 93.0 mol%, after 240
371 min. When the temperature was raised to 70 °C, the maximum of the BHMF yield (90.0
372 mol%) shifted to shorter reaction time (120 min), and then it strongly decreased by
373 prolonging the reaction. The further increase of the reaction temperature, first to 100 °C
374 and then to 120 °C, promoted the BHMF decomposition, as confirmed also by the
375 progressive decrease of carbon balance (runs 13 and 14, Table S2).

376 Therefore, the highest BHMF yield (93.0 mol%) was reached on 3 wt% HMF aqueous
377 solution at 50 °C, 30 bar H₂, and after 240 min, with a Ru/HMF ratio of 1 wt% (run 11).
378 In the literature, analogous BHMF yields are reported starting from aqueous HMF
379 solutions only employing significantly less sustainable reaction conditions
380 [27,45,46,57].

381 3.3 Hydrogenation of crude HMF-rich hydrolyzate obtained from fructose dehydration

382 The synthesis of BHMF and BHMTHF starting from pure HMF is scarcely attractive in
383 an industrial perspective due to the high cost of HMF, caused by its low yield in both
384 production and purification steps. On this basis, the hydrogenation of a crude HMF-rich
385 hydrolyzate was also investigated, thus evaluating the effect of other compounds, which

386 are typical of a real HMF-rich hydrolyzate, on the catalytic performances towards the
387 next HMF hydrogenation step. The hydrolyzate was obtained from the dehydration of
388 fructose, according to our previous work, in the presence of the commercial resin
389 Amberlyst-70 as acid catalyst, and the best HMF yield of 45.6 mol% was reached [13].
390 At the end of the hydrolysis reaction, the catalyst was separated by filtration and the
391 hydrolyzate was composed of 3 wt% of HMF, 2 wt% of unreacted fructose, 0.08 wt%
392 of formic acid and 0.15 wt% of levulinic acid, showing a pH=2.6, due to the significant
393 presence of the organic acids. This real hydrolyzate was subjected to hydrogenation at
394 100 °C and 50 bar H₂ (Figure 3, run 15).

395 Figure 3, near here

396 Comparing the above reaction profile with that of the hydrogenation of pure HMF,
397 which was carried out under the same reaction conditions (run 9, Table 2), it is evident
398 that, starting from the real hydrolyzate, the HMF conversion and the yields of the diols
399 were significantly lower than those achieved starting from pure HMF. This is due to the
400 significant formation of by-products, as confirmed by the very low carbon balance (run
401 15, Table S3). These include the unconverted fructose, rehydration acids, formic and
402 levulinic ones, and soluble humins. In order to verify the influence of these compounds
403 on the hydrogenation performances, some model mixtures, having the typical
404 concentrations of the raw hydrolyzate, were prepared, thus separately investigating the
405 effect of the addition of these components on the HMF hydrogenation. In this regard,
406 four model mixtures were prepared and hydrogenated: 1) HMF (3 wt%) with fructose (2
407 wt%) (Figure 4A, run 16); 2) HMF (3 wt%) with formic acid (0.08 wt%) and levulinic
408 acid (0.15 wt%) (Figure 4B, run 17); 3) HMF (3 wt%) with formic acid (0.08 wt%)
409 (Figure 4C, run 18); 4) HMF (3 wt%) with levulinic acid (0.15 wt%) (Figure 4D, run
410 19).

411 Figure 4, near here

412 The HMF hydrogenation in the presence of fructose (Figure 4A) proceeded similarly to
413 that of pure HMF (run 10, Table 2), showing that the presence of the unreacted
414 monosaccharide had no influence on the cascade reaction. On the contrary, formic and
415 levulinic acids had a detrimental effect on the hydrogenation of HMF, causing a
416 significant decrease of the reaction rate and a marked drop of BHMF and BHMTHF
417 yields, which respectively reached only 10 and 5 mol% after 30 and 120 min,
418 respectively (Figure 4B). As before evidenced, this result is in agreement with the
419 literature. In fact, not only the acid conditions promote the decomposition of the furan
420 diols [30,57], but it is known the strong deactivating adsorption of formic acid, which
421 remained in the reaction mixture because its decomposition to CO/CO₂ was not
422 significant under the adopted mild conditions [63]. This peculiar behaviour of formic
423 acid was also confirmed comparing the catalyst performances in the hydrogenation of
424 the HMF model mixtures with formic (Figure 4C) or levulinic acids (Figure 4D). In
425 fact, in the presence of formic acid, the conversion of HMF was slower than that found
426 in the HMF hydrogenation with levulinic acid. This is in agreement with the literature
427 results, already reported for the hydrogenation of levulinic acid, where it is underlined
428 that formic acid can be easily and strongly adsorbed on Ru particles in its formate form,
429 limiting the availability of the active sites for the substrate [63-65]. The deactivation of
430 the catalyst, due to the presence of formic acid, was also evidenced by the products
431 formation. In fact, in Figure 4C the conversion of HMF did not lead to diols but rather
432 to other by-products, indicating that the hydrogenation of HMF was strongly limited.
433 On the other hand, in the presence of levulinic acid (Figure 4D), considerable amount of
434 BHMF was obtained at short reaction time, proving that the HMF hydrogenation
435 occurred, but the acidity of the mixture had a detrimental effect with prolonging the
436 reaction, causing the decreasing of the furan diols yields. Moreover, the formation of
437 humins, deriving from HMF acid condensation [12,13,66], contributed to the catalyst

438 surface passivation [67]. Their formation was confirmed by the very low carbon balance
439 ascertained during the whole reaction in the presence of rehydration acids (runs 17, 18
440 and 19, Table S3). However, the conversion of HMF reached in the raw hydrolyzate
441 was even lower than that starting from the model mixtures of HMF with rehydration
442 acids, due to the presence of soluble humins already present in the raw hydrolyzate.
443 In order to overcome this drawback, the raw hydrolyzate was neutralized with NaHCO₃
444 until pH = 7, and then subjected to hydrogenation at 100 °C and 50 bar H₂ (Figure 5).

445 **Figure 5, near here**

446 The neutralization gave an improvement of the catalytic performances, and the BHMF
447 yield markedly improved, reaching the value of 73.2 mol% respect to the starting
448 amount of HMF. This value corresponds to a BHMF yield of 33.4 mol% respect to the
449 starting fructose employed in this cascade approach, being the yields of HMF from
450 fructose in the hydrolysis step equal to 45.6 mol% [13]. However, comparing this run
451 with the hydrogenation of pure HMF (run 9, Table 2), HMF conversion (Figure 5) and
452 the carbon balance (run 20, Table S3) for the neutralized hydrolyzate resulted still
453 lower, and the major product was BHMF, instead of BHMTHF, underlining that the
454 hydrogenation reaction remained almost limited. This evidence can be justified taking
455 into account that the neutralizing step counteracted the acid conditions, responsible for
456 the ring opening by-products and further humins formation in the hydrogenation step,
457 but the passivation effect of soluble humins already present in the hydrolyzate
458 remained, thus limiting the hydrogenation reaction [67].

459 **Regarding the reaction mechanism of HMF hydrogenation, it is well-known in the**
460 **literature that Ru-based catalysts favor the hydrogenation of C=O to give 2,5-**
461 **bis(hydroxymethyl)furan at relatively low temperatures, which would further be**
462 **converted to 2,5-dimethylfuran via hydrogenolysis, occurring at relatively high**
463 **temperatures, with 5-methylfurfuryl alcohol and 2,5-hexanedione as intermediate and**

464 by-product, respectively [68]. Moreover, regarding the reactivity of HMF, literature
465 studies on aldehydes have shown that decarbonylation path takes place on metals of
466 groups 8, 9, and 10, including ruthenium, especially at high temperatures, leading to the
467 formation of furfuryl alcohol and CO [60]. On the basis of our data, in order to
468 experimentally confirm the HMF hydrogenation mechanism as the main one
469 responsible for the production of BHMF and BHMTHF performed under mild reaction
470 conditions, 50 °C, 30 bar H₂ and 100 °C, 50 bar H₂ respectively, the reaction mixtures
471 obtained under these conditions starting from pure HMF were analysed by GC-MS and
472 the gas-phase reaction products by GC analysis. Only trace amounts of products
473 deriving from hydrogenolysis or decarbonylation reactions of HMF and/or of BHMF,
474 and/or from subsequent hydrogenation/hydrogenolysis reactions on the obtained
475 hydrogenolysis or decarbonylation products were detected (Figure S4 and S5). These
476 products can include 5-methylfurfural, furfuryl alcohol, 5-methylfurfuryl alcohol, 5-
477 methyltetrahydrofurfuryl alcohol, 2,5-dimethyltetrahydrofuran, tetrahydrofurfuryl
478 alcohol, some of which were present in low amounts (not negligible) when the reaction
479 was performed at 140 °C, 70 bar H₂, as already reported in Figure S2, confirming that
480 hydrogenolysis and decarbonylation pathways become more important at high
481 temperatures. Also in the gas-phase, only trace amounts of CO were detected, in
482 agreement with the literature, highlighting as the hydrogenation mechanism is the main
483 one for ruthenium catalysts in the production of BHMF and BHMTHF from HMF [68].
484 In this regard, it is reasonable that, when the C=O hydrogenation is the main reaction
485 pathway, the preferential HMF adsorption mode on the active metal occurs in the
486 $\eta^2(\text{C},\text{O})$ -aldehyde configuration. By this way, BHMF could be selectively formed from
487 this $\eta^2(\text{C},\text{O})$ species,. Once BHMF was obtained in the reaction mixture, this molecule
488 may be adsorbed in two different modes for the subsequent hydrogenation step: parallel
489 and tilted. The parallel mode may lead to complete hydrogenation, forming BHMTHF,

490 whereas the tilted one may cause the ring opening, through the C-O bond cleavage, with
491 the final formation of 1,2,6-hexanetriol, after hydrogenation step. This proposed
492 mechanism is reported in the Scheme 2, and it is in agreement with the literature data
493 [59,60].

494 **Scheme 2, near here**

495 In order to better evaluate the amount of carbonaceous material on the catalyst surface
496 at the end of the reaction and how it affects the physical properties of the employed
497 catalyst, TGA (Figure 6) and N₂ physisorption (Figure S6 and Table S4) analyses were
498 carried out on fresh and spent Ru/C catalysts at the end of hydrogenation reactions
499 performed adopting different starting materials: solutions of pure HMF (run 9, Table 2),
500 the raw hydrolyzate (run 15, Figure 3) and the neutralized one (run 20, Figure 5).

501 **Figure 6, near here**

502 **Figure 6** shows that the amount of carbonaceous material (humins) on the spent
503 catalysts is strongly influenced by the type of the starting substrate. In fact, when the
504 raw hydrolyzate was employed as starting material, the lowest residual weight was
505 acquired at the end of the analysis, confirming that, in this case, the highest amount of
506 humins was deposited on the catalyst, originating from both the crude hydrolyzate and
507 the HMF condensation that took place during the hydrogenation reaction. The
508 neutralizing step allowed the reduction of humins formation, thus the residual weight
509 recorded at the end of the analysis was higher than that obtained for the crude
510 hydrolyzate, but lower than that for the catalyst employed in the hydrogenation of pure
511 HMF. This explains the trend found for HMF conversion and it is in agreement with the
512 **N₂ physisorption experiments** reported in **Figure S6** and **Table S4**. In fact, the
513 isothermal curves and the specific surface area values show that the surface area of the
514 spent catalysts depend on the adopted substrate, following this order: pure HMF (153
515 **m²/g**) > neutralized hydrolyzate (62 **m²/g**) > raw hydrolyzate (6 **m²/g**), being equal to

516 770 m²/g that of fresh Ru/C system. The catalyst support plays a significant influence on
517 the catalytic activity in the selective hydrogenation of HMF. The obtained catalytic
518 trend is in agreement with the literature: supports with high surface area favor the
519 dispersion of active metal particles on their surfaces, providing more active catalytic
520 sites for the hydrogenation reactions [36]. Moreover, it is evident that the surface area
521 of the catalyst recovered after the hydrogenation of pure HMF was lower than that of
522 the fresh Ru/C, indicating that, also in this case, some organic material could be
523 adsorbed on the catalyst surface, as previously observed by the comparison of the
524 thermogravimetric curves of these two catalysts reported in Figure 6.

525 In order to improve the yields towards BHMTHF starting from the crude HMF, harsher
526 reaction conditions (140 °C, 70 bar H₂) were adopted, and the results are shown in
527 Figure 7 (run 21).

528 **Figure 7, near here**

529 **Both** HMF conversion and carbon balance were similar to those obtained working at
530 100 °C and 50 bar H₂, but the product distribution significantly changed. In fact, in this
531 case, the prevailing furan diol resulted BHMTHF, which after 240 min reached the yield
532 of 81.1 mol% respect to the amount of initial HMF present in the hydrolyzate, which
533 corresponds to the value of 37.0 mol% respect to the starting fructose, taking into
534 account that in the first step the yield of HMF starting from fructose was 45.6 mol%
535 [13].

536 Up to now, only few papers report the synthesis of these diols directly from fructose
537 [31,50,69,70]. However, to the best of our knowledge, in this work, for the first time,
538 both fructose dehydration and hydrolyzate hydrogenation were carried out in water
539 instead of organic solvents, ionic liquids or organic-water mixtures. In particular, the
540 first step of this cascade approach is the most critical, due to the possible decomposition
541 of HMF to humins and rehydration acids, which causes the lowering of the HMF yield

542 respect to those obtained with different solvent systems, which **should** allow an almost
543 quantitative HMF yield [7]. Therefore, in the second step (HMF hydrogenation), the
544 literature investigations performed in organic solvent **are based on hydrolyzates which**
545 **don't include the presence of rehydration acids and humins**, thus allowing the
546 maximization of the **furan** diols yields. However, the employment of organic media or
547 ionic liquid makes the literature processes significantly less sustainable under economic,
548 environmental and safety points of view.

549 *3.4 Catalyst stability*

550 When a heterogeneous catalyst is employed, the evaluation of its stability is an essential
551 issue. For this purpose, the fresh and spent Ru/C catalysts recovered at the end of the
552 optimized reactions for the synthesis of both BHMTHF (run 9, **Table 2**) and BHMF
553 (run 11, Figure 2), **both** starting from pure HMF were analysed through ICP-OES and
554 TEM techniques. The first one proved that the leaching of ruthenium in the solution was
555 negligible when it was employed **for** the synthesis of BHMF and BHMTHF. The TEM
556 pictures and the distributions of the ruthenium particles size for the fresh and the spent
557 Ru/C catalysts are reported in **Figure 8**.

558 **Figure 8, near here**

559 The TEM image of fresh Ru/C catalyst shows that this system is characterized by
560 ruthenium particles with very small average size, 1.5 nm, in agreement with the results
561 reported in the literature [71]. **On the other hand, the ruthenium particles sizes in the**
562 **spent catalysts were 2.5 and 2.3 nm, for those employed for the synthesis of BHMTHF**
563 **and BHMF, respectively**. In order to investigate the recyclability of the catalyst, the
564 catalytic system employed in run 9 (**Table 2**) was recovered at the end of the reaction by
565 filtration, and reused in two subsequent tests, using the same reaction conditions
566 adopted in run 9. The obtained results are reported in **Figure 9**.

567 **Figure 9, near here**

568 During these three cycles (1, 2 and 3), a slight decrease of the catalytic activity was
569 observed. In fact, the HMF conversion was not complete in the recycling runs and, after
570 the third one, a decrease of 13.8 mol% was obtained. Moreover, a modest increase of
571 BHMF yield (4.2 mol% in the third cycle) was observed, due to the passivation of
572 catalyst surface. At the end of the third cycle, the recovered catalyst was washed with
573 acetone, dried and reused again in another subsequent recycling test. After the washing
574 treatment, the catalyst performances were almost entirely restored, proving that the
575 increase of ruthenium particle sizes did not influence the catalytic activity and
576 confirming that the adopted washing treatment represents an efficient and simple
577 reactivation method, able to remove humins from catalyst surface.

578 These results underline that catalytic performances of the Ru/C catalyst can be restored,
579 in agreement with our previous research on hydrogenation of raw biomass-derived
580 levulinic acid to γ -valerolactone (GVL) [65], or to 2-methyltetrahydrofuran, and to 2-
581 butanol [72]. The prevailing deactivation of the catalyst can be related only to humin
582 deposition on the surface, which could be removed through washing and/or thermal
583 treatments.

584 **4. Conclusion**

585 Ru/C, Pd/C and Pt/C catalysts were studied in the hydrogenation of pure HMF aqueous
586 solutions to obtain the furan diols 2,5-bis(hydroxymethyl)furan (BHMF) and 2,5-
587 bis(hydroxymethyl)tetrahydrofuran (BHMTHF). Under the same reaction conditions,
588 Pt/C and Pd/C promoted the HMF hydrodeoxygenation and ring opening, whereas Ru/C
589 mainly activated the HMF hydrogenation, thus resulting as the best catalyst, in terms of
590 conversion and selectivity, towards the desired products. The investigation on Ru/C
591 catalyst revealed that mild reaction conditions were appropriate for obtaining high
592 BHMF yield, whereas higher temperature and H₂ pressure were necessary to
593 hydrogenate also the furan ring, thus selectively obtaining BHMTHF. From the

594 composition of the reaction mixtures, in terms of ascertained by-products, informations
595 on the reaction mechanism were inferred. The hydrogenation of HMF-rich hydrolyzate
596 obtained from the dehydration of fructose aqueous solution was subsequently studied.
597 The investigation evidenced the detrimental role of formic and levulinic acids, which
598 promote the formation of ring opening by-products and humins, which can passivate the
599 catalyst surface. However, the neutralization of the hydrolyzate allowed the
600 improvement of the catalyst performances, preventing the humins formation, as
601 confirmed by N₂ physisorption and TGA analyses of spent catalysts. These results
602 evidence, for the first time, the feasibility of the BHMF and BHMTFH synthesis with
603 good yields, starting from aqueous crude HMF and commercial Ru/C catalyst.
604 Moreover, the recycling data obtained in batch reactor are promising and experiments in
605 continuous set-up are now in progress in order to investigate the catalyst performances
606 for long time on stream.

607

608 **References**

- 609 [1] I.K.M. Yu, D.C.W. Tsang, *Biores. Technol.* 238 (2017) 716-732.
- 610 [2] C. Antonetti, D. Licursi, S. Fulignati, G. Valentini, A.M. Raspolli Galletti, *Catalysts*
611 6 (2016) 196-224.
- 612 [3] L. Hu, L. Lin Z. Wu, S. Zhou, S. Liu, *Renew. Sust. Energ. Rev.* 74 (2017) 230-257.
- 613 [4] D.P. Serrano, J.A. Melero, G. Morales, J. Iglesias, P. Pizarro, *Catal. Rev.* 60 (2018)
614 1-70.
- 615 [5] C. Antonetti, E. Bonari, D. Licursi, N. Nassi o Di Nasso, A.M. Raspolli Galletti,
616 *Molecules* 20 (2015) 21232-21253.
- 617 [6] A. Galia, B. Schiavo, C. Antonetti, A.M. Raspolli Galletti, L. Interrante, M. Lessi,
618 O. Scialdone, M.G. Valenti, *Biotechnol. Biofuels* 8 (2015) 218-236.
- 619 [7] S.P. Teong, G. Yi, Y. Zhang, *Green Chem.* 16 (2014) 2015-2026.

- 620 [8] M. Li, W. Li, Y. Lu, H. Jameel, H. Chang, L. Ma, *RSC Adv.* 7 (2017) 14330-14336.
- 621 [9] B. Agarwal, K. Kailasam, R.S. Sangwan, S., Elumalai, *Renew. Sust. Ener. Rev.*, 82
622 (2018) 2408-2425.
- 623 [10] A.A. Marianou, C.M. Michailof, A. Pineda, E.F. Iliopoulou, K.S. Triantafyllidis,
624 A.A. Lappas, *Appl. Catal. A: Gen.* 555 (2018) 75-87.
- 625 [11] L. Atanda, A. Shrotri, S. Mukundan, Q. Ma, M. Konarova, J. Beltramini,
626 *ChemSusChem* 8 (2015) 2907-2916.
- 627 [12] C. Antonetti, M. Melloni, D. Licursi, S. Fulignati, E. Ribechini, S. Rivas, J.C.
628 Parajó, F. Cavani, A.M. Raspolli Galletti, *Appl. Catal. B: Env.* 206 (2017) 364-
629 377.
- 630 [13] C. Antonetti, A.M. Raspolli Galletti, S. Fulignati, D. Licursi, *Catal. Commun.* 97
631 (2017) 146-150.
- 632 [14] A.N. Chermahini, H. Hafizi, N. Andisheh, M. Saraji, A. Shahvar, *Res. Chem.*
633 *Intermed.* 43 (2017) 5507-5521.
- 634 [15] I.A. Masiutin, A.A. Novikov, A.A. Litvin, D.S. Kopitsyn, D.A. Beskorovaynaya,
635 E.V. Ivanov, *Starch/Stärke* 68 (2016) 637-643.
- 636 [16] X. Qi, M. Watanabe, T.M. Aida, R.L. Smith Jr., *Green Chem.* 12 (2010) 1855-
637 1860.
- 638 [17] H. Shirai, S. Ikeda, E.W. Qian, *Fuel Process. Technol.* 159 (2017) 280-286.
- 639 [18] R. Weingarten, A. Rodriguez-Beuerman, F. Cao, J.S. Lutherbacher, D.M. Alonso,
640 J.A. Dumesic, G.W. Huber, *ChemCatChem* 6 (2014) 2229-2234.
- 641 [19] Y. Yang, C.W. Hu, M.M. Abu-Omar, *ChemSusChem* 5 (2012) 405-410.
- 642 [20] M.J. Gilkey, D.G. Vlachos, B. Xu, *Appl. Catal. A: Gen.* 542 (2017) 327-335.
- 643 [21] J. Li, J. Liu, H. Liu, G. Xu, J. Zhang, J. Liu, G. Zhou, Q. Li, Z. Xu, Y. Fu,
644 *ChemSusChem* 10 (2017) 1436-1447.

- 645 [22] G. Raveendra, A. Rajasekhar, M. Srinivas, P.S. Sai Prasad, N. Lingaiah, Appl.
646 Catal. A: Gen. 520 (2016) 105-113.
- 647 [23] B.O. De Beeck, M. Dusselier, J. Geboers, J. Holsbeek, E. Morré, S. Oswald, L.
648 Giebeler, B.F. Sels, Energy Environ. Sci. 8 (2015) 230-240.
- 649 [24] G. Yi, S.P. Teong, Y. Zhang, Green Chem. 18 (2016) 979-983.
- 650 [25] D.X. Martínez-Vargas, J.R. De La Rosa, L. Sandoval-Rangel, J.L. Guzmán-Mar,
651 M.A. Garza-Navarro, C.J. Lucio-Ortiz, D.A. De Haro-Del Río, Appl. Catal. A:
652 Gen. 547 (2017) 132-145.
- 653 [26] G. Bottari, A.J. Kumalaputri, K.K. Krawczyk, B.L. Feringa, H.J. Heeres, K. Barta,
654 ChemSusChem 8 (2015) 1323-1327.
- 655 [27] M. Chatterjee, T. Ishizaka, H. Kawanami, Green Chem. 16 (2014) 4734-4739.
- 656 [28] J.J. Roylance, T.W. Kim, K. Choi, ACS Catal. 6 (2016) 1840-1847.
- 657 [29] N. Perret, A. Grigoropoulos, M. Zanella, T.D. Manning, J.B. Claridge, M.J.
658 Rosseinsky, ChemSusChem 9 (2016) 521-531.
- 659 [30] R. Alamillo, M. Tucker, M. Chia, Y. Pagán-Torres, J. Dumesic, Green Chem. 14
660 (2012) 1413-1419.
- 661 [31] H. Cai, C. Li, A. Wang, T. Zhang, Catal. Today 234 (2014) 59-65.
- 662 [32] T. Buntara, S. Noel, P.H. Phua, I. Melián-Cabrera, J.G. De Vries, H.J. Heeres,
663 Angew. Chem. Int. Ed. 50 (2011) 7083-7087.
- 664 [33] T. Buntara, I. Melián-Cabrera, Q. Tan, J.L.G. Fierro, M. Neurock, J.G. De Vries,
665 H.J. Heeres, Catal. Today 210 (2013) 106-116.
- 666 [34] K. Gupta, R.K. Rai, S.K. Singh, ChemCatChem 10 (2018) 2326-2349
- 667 [35] B. Ma, Y. Wang, X. Guo, X. Tong, C. Liu, Y. Wang, X. Guo, Appl. Catal. A: Gen.
668 552 (2018) 70-76.
- 669 [36] X. Tang, J. Wei, N. Ding, Y. Sun, X. Zeng, L. Hu, S. Liu, T. Lei, L. Lin, Renew.
670 Sust. Ener. Rev. 77 (2017) 287-296.

- 671 [37] M. Gomes, A. Gandini, A.J.D. Silvestre, B. Reis, *J. Polym. Sci. Part A: Polym.*
672 *Chem.* 49 (2011) 3759-3768.
- 673 [38] D. Zhang, M. Dumont, *J. Polym. Sci., Part A: Polym. Chem.* 55 (2017) 1478-1492.
- 674 [39] L. Hu, J. Xu, S. Zhou, A. He, X. Tang, L. Lin, J. Xu, Y. Zhao, *ACS Catal.* 8 (2018)
675 2959-2980.
- 676 [40] A. Gandini, T.M. Lacerda, A.J.F. Carvalho, E. Trovatti, *Chem. Rev.* 116 (2016)
677 1637-1669.
- 678 [41] T. Thananathanachon, T.B. Rauchfuss, *ChemSusChem* 3 (2010) 1139-1141.
- 679 [42] T. Wang, J. Zhang, W. Xie, Y. Tang, D. Guo, Y. Ni, *Catalysts* 7 (2017) 92-99.
- 680 [43] L. Hu, M. Yang, N. Xu, J. Xu, S. Zhou, X. Chu, Y. Zhao, *Korean J. Chem. Eng.* 35
681 (2018) 99-109.
- 682 [44] T. Pasini, G. Solinas, V. Zanotti, S. Albonetti, F. Cavani, A. Vaccari, A. Mazzanti,
683 S. Ranieri, R. Mazzoni, *Dalton Trans.* 43 (2014) 10224-10234.
- 684 [45] J. Ohyama, A. Esaki, Y. Yamamoto, S. Arai, A. Satsuma, *RSC Adv.* 3 (2013)
685 1033-1036.
- 686 [46] J. Chen, F. Lu, J. Zhang, W. Yu, F. Wang, J. Gao, J. Xu, *ChemCatChem* 5 (2013)
687 2822-2826.
- 688 [47] J. Han, Y.H. Kim, H.S. Jang, S.Y. Hwang, J. Jegal, J.W. Kim, Y.S. Lee, *RSC Adv.*
689 6 (2016) 93394-93397.
- 690 [48] J. Chen, R. Liu, Y. Guo, L. Chen, H. Gao, *ACS Catal.* 5 (2015) 722-733.
- 691 [49] Y. Nakagawa, K. Takada, M. Tamura, K. Tomishige, *ACS Catal.* 4 (2014) 2718-
692 2726.
- 693 [50] P.P. Upare, Y.K. Hwang, D.W. Hwang, *Green Chem.* 20 (2018) 879-885.
- 694 [51] Y. Zhu, X. Kong, H. Zheng, G. Ding, Y. Zhu, Y.W. Li, *Catal. Sci, Technol.* 5
695 (2015) 4208-4217.

696 [52] X. Kong, Y. Zhu, H. Zheng, F. Dong, Y. Zhu, Y.W. Li, RSC Adv. 4 (2014) 60467-
697 60472.

698 [53] S. Chen, R. Wojcieszak, F. Dumeignil, E. Marceau, S. Royer, Chem. Rev. 18
699 (2018) 11023–11117.

700 [54] F. Liu, M. Audemar, K. De Oliveira Vigier, J.M. Clacens, F. De Campo, F.
701 Jérôme, Green Chem. 16 (2014) 4110-4114.

702 [55] X. Hu, S. Kadarwati, Y. Song, C.Z. Li, RSC Adv. 6 (2016) 4647-4656.

703 [56] Y. Nakagawa, K. Tomishige, Catal. Commun. 12 (2010) 154-156.

704 [57] V. Schiavo, G. Descotes, J. Mentech, Bull. Soc. Chim. Fr. 128 (1991) 704-711.

705 [58] J. Luo, L. Arroyo-Ramirez, R.J. Gorte, AIChE 61 (2015) 590-597.

706 [59] S. Yao, X. Wang, Y. Jiang, F. Wu, X. Chen, X. Mu, ACS Sustainable Chem. Eng.
707 2 (2014) 173-180.

708 [60] D.P. Duarte, R. Martínez, L.J. Hoyos, Ind. Eng. Chem. Res. 55 (2016) 54-63.

709 [61] J. Mitra, X. Zhou, T. Rauchfuss, Green Chem. 17 (2015) 307-313.

710 [62] B. Zhang, Y. Zhu, G. Ding, H. Zheng, Y. Li, Green Chem. 14 (2012), 3402-3409.

711 [63] H. Heeres, R. Handana, D. Chunai, C.B. Rasrendra, B. Girisuta, H.J. Heeres, Green
712 Chem. 11 (2009) 1247-1255.

713 [64] A.M. Ruppert, M. Jędrzejczyk, O. Sneka-Płatek, N. Keller, A.S. Dumon, C.
714 Michel, P. Sautet, J. Grams, Green Chem. 18 (2016) 2014–2028.

715 [65] S. Rivas, A.M. Raspolli Galletti, C. Antonetti, D. Licursi, V. Santos, J.C. Parajó,
716 Catalysts 8 (2018) 169-184.

717 [66] G. Tsilomelekis, M.J. Orella, Z. Lin, Z. Cheng, W. Zheng, V. Nikolakis, D.G.
718 Vlachos, Green Chem. 18 (2016) 1983-1993.

719 [67] Y. Yang, Q. Liu, D. Li, J. Tan, Q. Zhang, C. Wang, L. Ma, RSC Adv. 7 (2017),
720 16311-16318.

721 [68] L. Hu, X. Tang, J. Xu, Z. Wu, L. Lin, S. Liu, *Ind. Eng. Chem. Res.* 53 (2014)
722 3056-3064.

723 [69] X. Xiang, J. Cui, G. Ding, H. Zheng, Y. Zhu, Y. Li, *ACS Sustainable Chem. Eng.*
724 4 (2016) 4506-4510.

725 [70] W. Zhao, W. Wu, H. Li, C. Fang, T. Yang, Z. Wang, C. He, S. Yang, *Fuel* 217
726 (2018) 365-369.

727 [71] S. Iqbal, S.A. Kondrat, D.R. Jones, D.C. Schoenmakers, J.K. Edwards, L. Lu, B.R.
728 Yeo, P.P. Wells, E.K. Gibson, D.J. Morgan, C.J. Kiely, G.J. Hutchings, *ACS*
729 *Catal.* 5 (2015) 5047-5059.

730 [72] D. Licursi, C. Antonetti, S. Fulignati, M. Giannoni, A.M. Raspolli Galletti,
731 *Catalysts* 8 (2018) 277-292.

732

733

734

735

736

737

738

739

740

741

742

743

744

745

746

747

748

749 **Caption for Figures and Schemes**

750 **Fig. 1.** Influence of temperature on the HMF aqueous hydrogenation in the presence of
751 5 wt% Ru/C carried out at 70 bar H₂ and: A) 140 °C (run 4); B) 120 °C (run 5), C) 100
752 °C (run 6). Reaction conditions: [HMF] = 2 wt%; Ru/HMF = 1 wt%; P H₂ = 70 bar.

753 **Fig. 2.** Influence of temperature on the HMF aqueous hydrogenation in the presence of
754 5 wt% Ru/C carried out at 30 bar H₂ and: 50 °C (run 11); 70 °C (run 12); 100 °C (run
755 13) and 120 °C (run 14). Reaction conditions: [HMF] = 3 wt%; Ru/HMF = 1 wt%; P H₂
756 = 30 bar.

757 **Fig. 3.** Profile of HMF aqueous hydrogenation of hydrolyzate in the presence of 5 wt%
758 Ru/C (run 15). Reaction conditions: [HMF] = 3 wt%; Ru/HMF = 1 wt%; T = 100 °C; P
759 H₂ = 50 bar.

760 **Fig. 4.** Profile of HMF aqueous hydrogenation in the presence of 5 wt% Ru/C of: A)
761 fructose + HMF (run 16); B) formic acid + levulinic acid + HMF (run 17); C) HMF +
762 formic acid (run 18); D) HMF + levulinic acid (run 19). Reaction conditions: [HMF] =
763 3 wt%; Ru/HMF = 1 wt%; T = 100 °C; P H₂ = 50 bar.

764 **Fig. 5.** Profile of HMF aqueous hydrogenation of neutralized hydrolyzate in the
765 presence of 5 wt% Ru/C (run 20). Reaction conditions: [HMF] = 3 wt%; Ru/HMF = 1
766 wt%; T = 100 °C; P H₂ = 50 bar.

767 **Fig. 6.** TGA analysis of fresh and spent Ru/C catalysts recovered at the end of the
768 hydrogenation reactions starting from different initial substrates: pure HMF (run 9,
769 Table 2), hydrolyzate (run 15, Figure 3) and neutralized hydrolyzate (run 20, Figure 5).
770 Reaction conditions: [HMF] = 3 wt%; Ru/HMF = 1 wt%; T = 100 °C; P H₂ = 50 bar; t =
771 240 min.

772 **Fig. 7.** Kinetic profile of neutralized hydrolyzate hydrogenation. Reaction conditions:
773 [HMF] = 3 wt%; Ru/HMF = 1 wt%; T = 140 °C; P H₂= 70 bar (run 21).

774 **Fig. 8.** TEM pictures of fresh Ru/C (A) and spent Ru/C catalysts employed in run 9,
775 Table 2 (B) or run 11 (C) with the respective distribution of the Ru particles sizes and
776 the Gaussian fitting.

777 **Fig. 9.** Hydrogenation of pure HMF in the presence of 5 wt% Ru/C (run 9, Table 2) and
778 four recycles of the solid catalyst.

779 **Scheme 1.** Pathways of HMF hydrogenation by-products formation in the presence of
780 the following catalysts: A) Pt/C; B) Ru/C and C) Pd/C.

781 **Scheme 2.** Mechanism of HMF hydrogenation.

782

783

784

785

786

787

788

789

790

791

792

793

794

795

796

797

798 **Table 1** Catalytic performances of commercial systems in the aqueous hydrogenation of
 799 HMF. Reaction conditions: [HMF] = 2 wt%; metal/HMF ratio = 1 wt%; T = 140 °C; P
 800 H₂= 70 bar; t = 60 min.

Run	Catalyst	HMF	BHMF	BHMF	BHMTHF	BHMTHF	Carbon
		Conversion (mol%)	Yield (mol%)	Selectivity (mol%)	Yield (mol%)	Selectivity (mol%)	balance (mol%)
1	Pt/C (5 wt%) ^a	64.5	10.7	16.6	0	0	46.2
2	Pd/C (5 wt%) ^b	100	0	0	55.8	55.8	55.8
3	Ru/C (5 wt%) ^c	100	0	0	88.6	88.6	88.6

801 ^a Main by-products: 5-methyl-2-furaldehyde; 2,5-hexanedione; 5-hydroxy-2-hexanone.

802 ^b Main by-products: tetrahydrofurfuryl alcohol; 5-methyl-tetrahydrofurfuryl alcohol;
 803 2,5-dimethyltetrahydrofuran; tetrahydro-2H-pyran-2-methanol.

804 ^c Main by-products: 5-methyl-tetrahydrofurfuryl alcohol; 2,5-hexanedione; 5-hydroxy-
 805 2-hexanone; 1,2,6-hexanetriol.

806

807

808

809

810

811

812

813

814

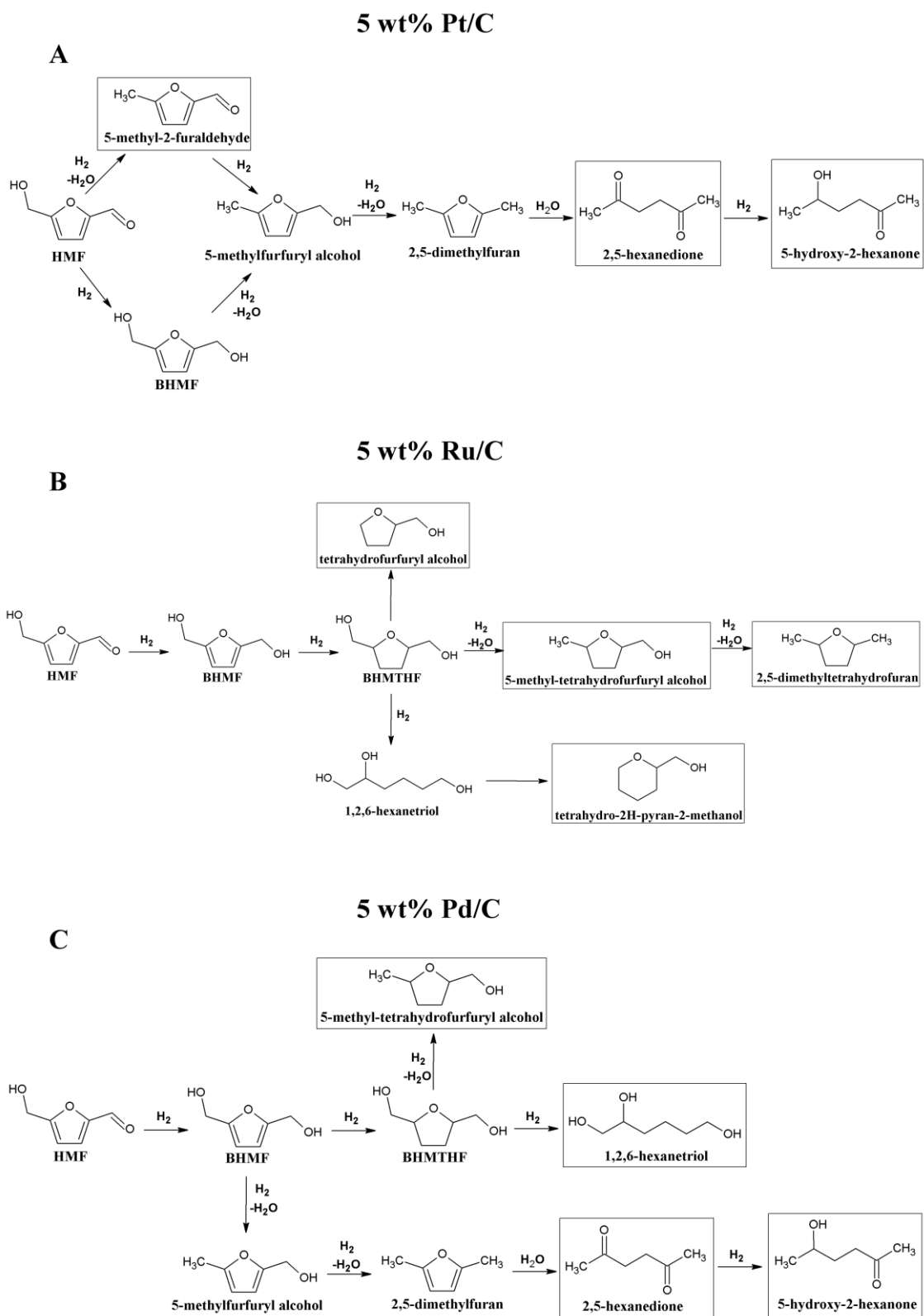
815

816

817

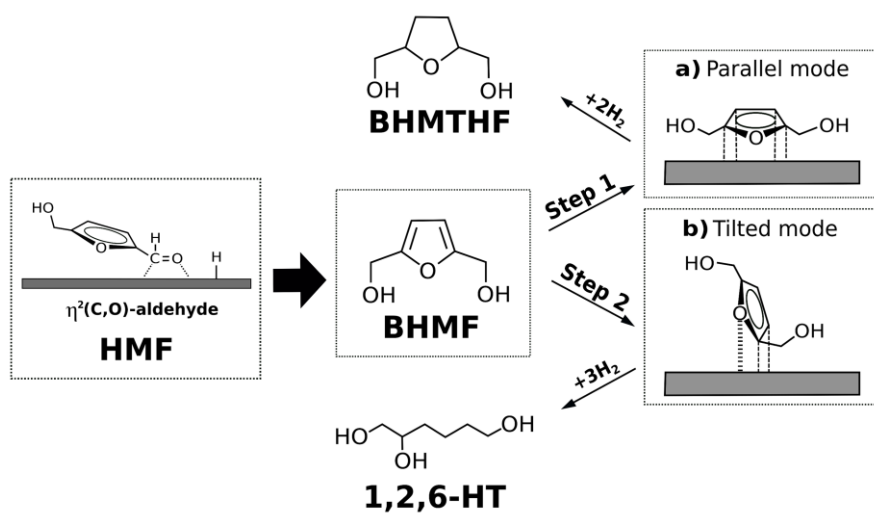
818 **Table 2** Influence of H₂ pressure and HMF concentration on the aqueous hydrogenation
 819 of HMF in the presence of 5 wt% Ru/C. Reaction conditions: Ru/HMF ratio = 1 wt%; T
 820 = 100 °C.

Run	P H ₂ (bar)	[HMF] (wt%)	HMF Conversion (mol%)				BHMTHF Yield (mol%)				Carbon Balance (mol%)							
			30	60	120	240	30	60	120	240	30	60	120	240				
			Time (min)															
7	70	2	97.0	100	100	100	22.2	0.0	0.0	0.0	69.3	87.0	90.1	95.3	94.5	87.0	90.1	95.3
8	50	2	96.8	100	100	100	32.0	0.0	0.0	0.0	59.2	89.3	91.8	93.3	94.4	89.3	91.8	93.3
9	50	3	96.8	100	100	100	71.3	16.9	0.0	0.0	25.0	71.5	92.0	95.3	99.5	88.4	92.0	95.3
10	30	3	89.5	98.4	100	100	79.5	64.4	21.2	0.0	2.9	6.1	19.2	29.6	92.9	72.1	40.4	29.6



826

Scheme 2



827

828

829

830

831

832

833

834

835

836

837

838

839

840

841

842

843

844

Figure 1

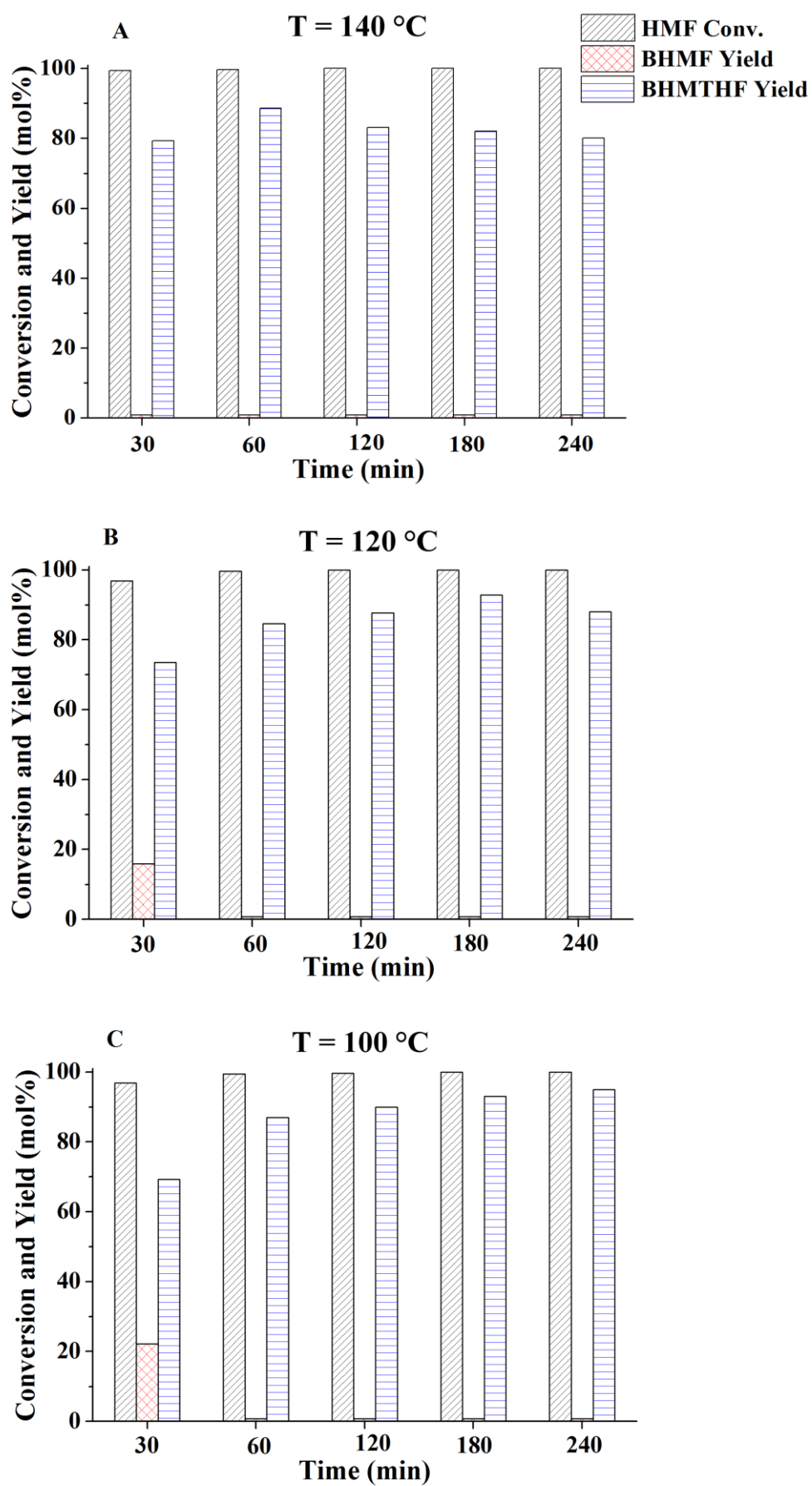


Figure 2

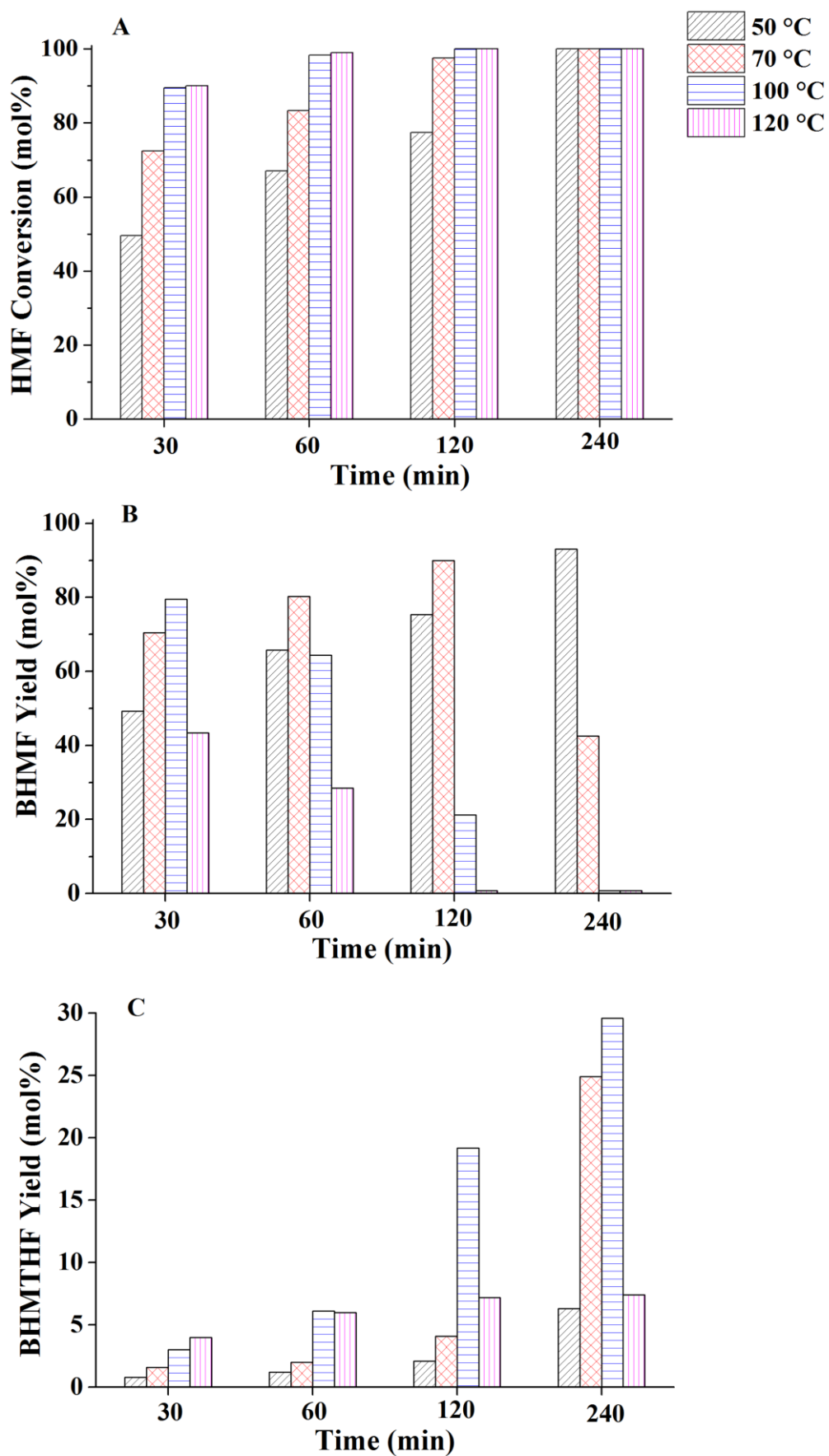
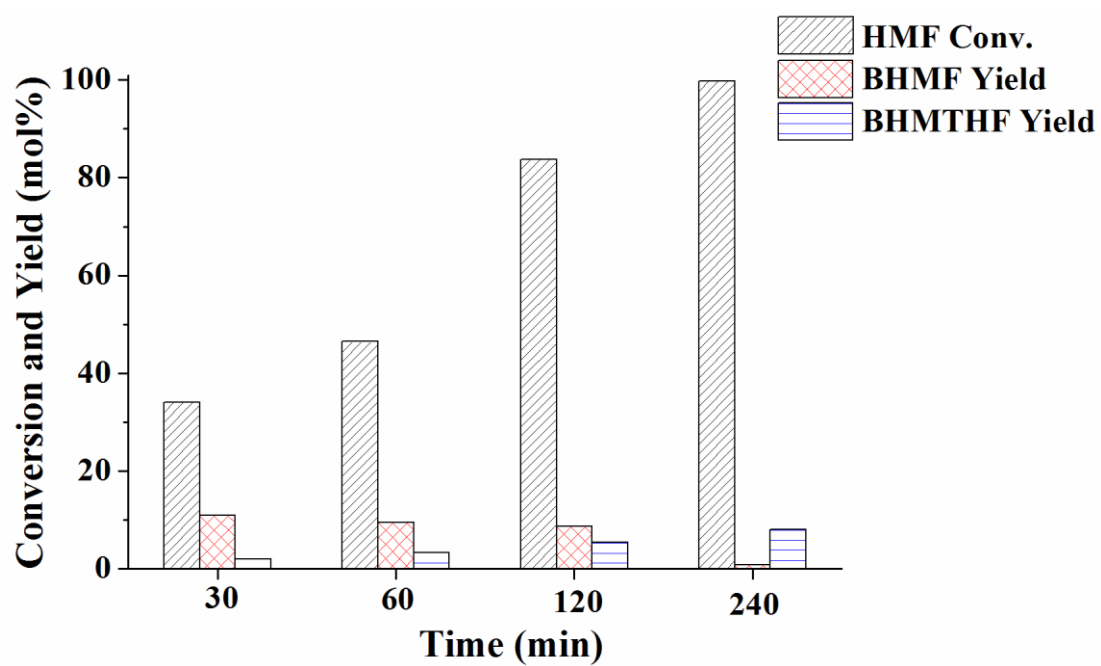


Figure 3



850

851

852

853

854

855

856

857

858

859

860

861

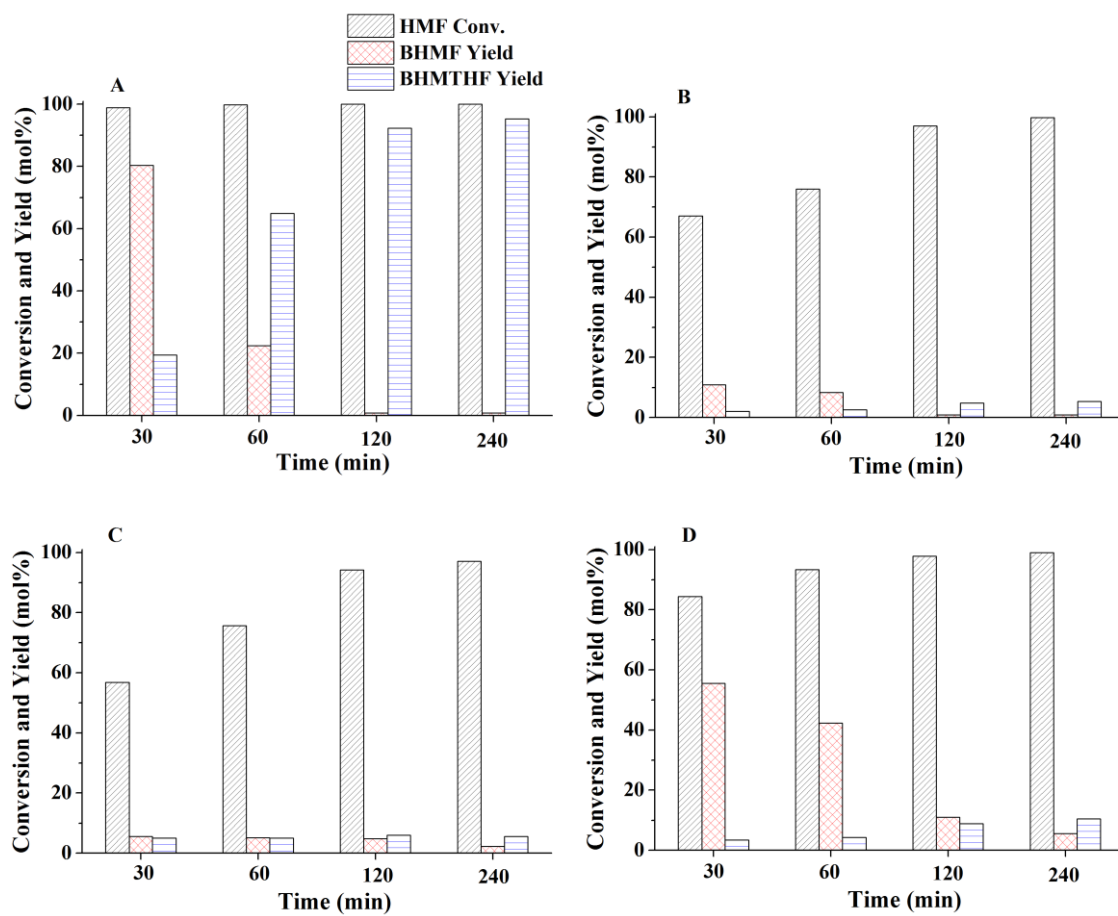
862

863

864

865

Figure 4



867

868

869

870

871

872

873

874

875

876

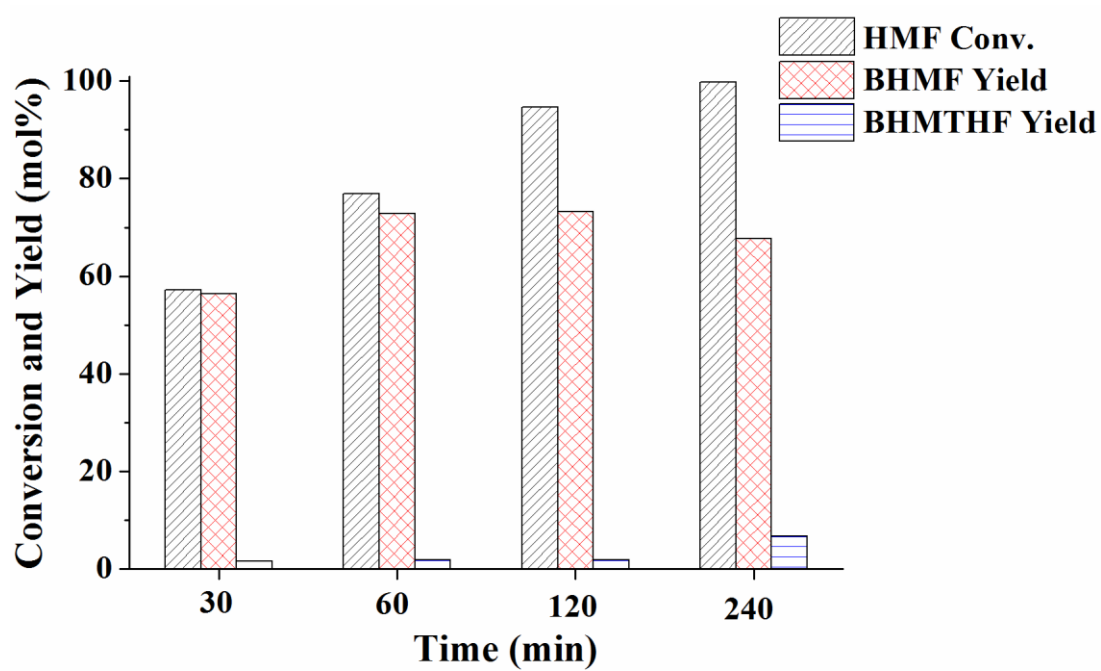
877

878

879

880

Figure 5



881

882

883

884

885

886

887

888

889

890

891

892

893

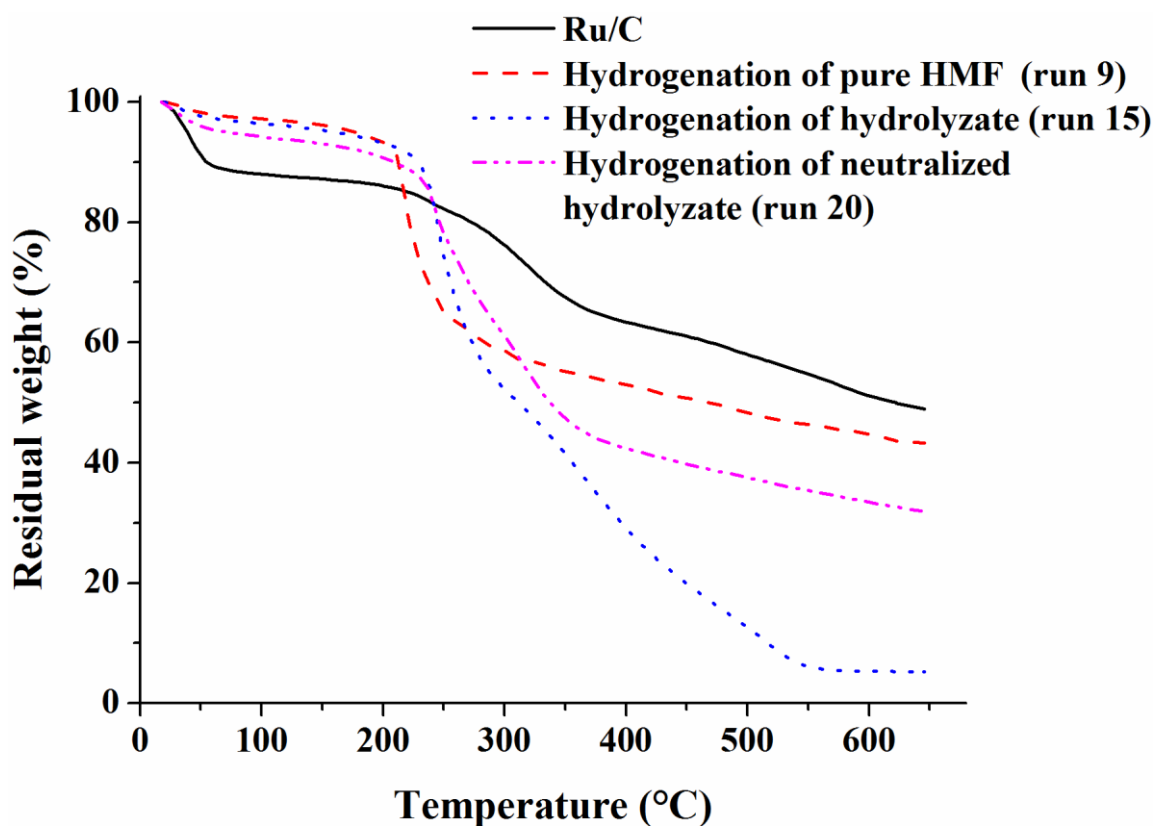
894

895

896

897

Figure 6



898

899

900

901

902

903

904

905

906

907

908

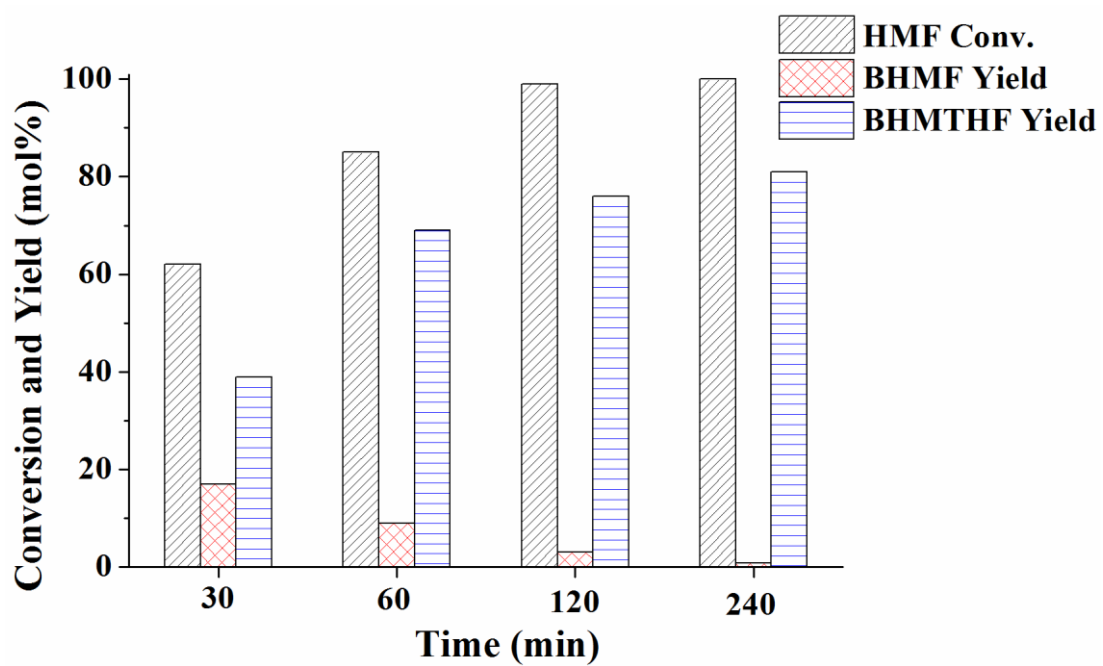
909

910

911

912

Figure 7



913

914

915

916

917

918

919

920

921

922

923

924

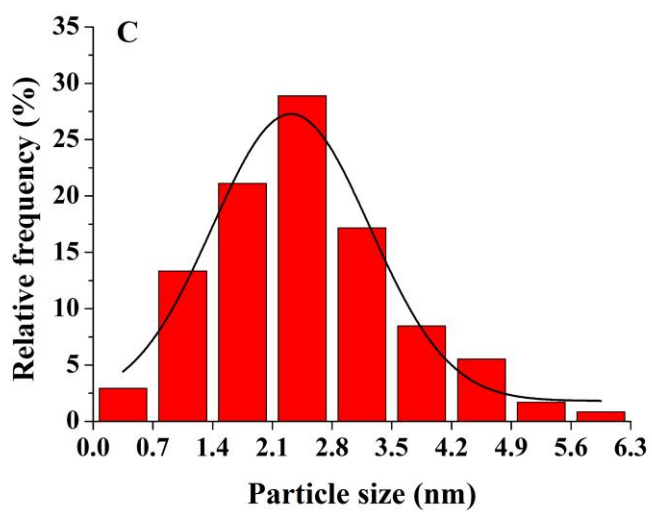
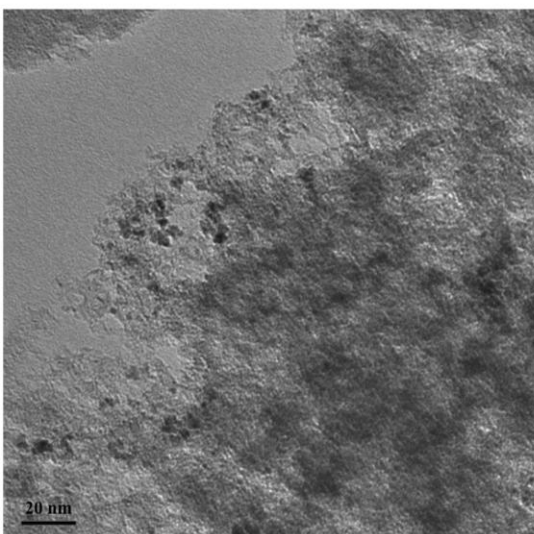
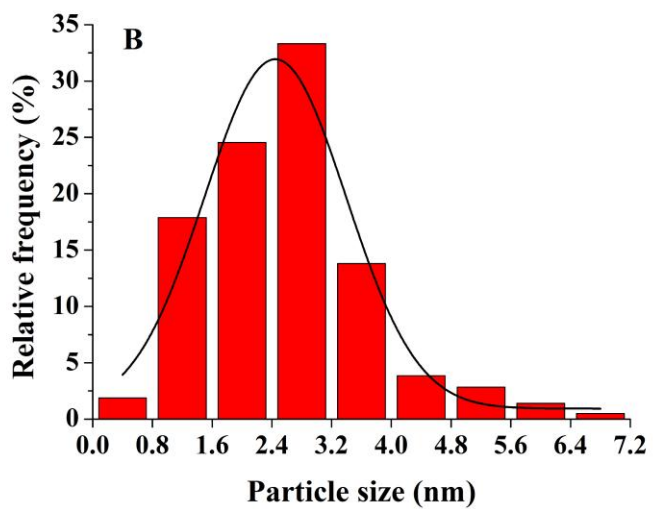
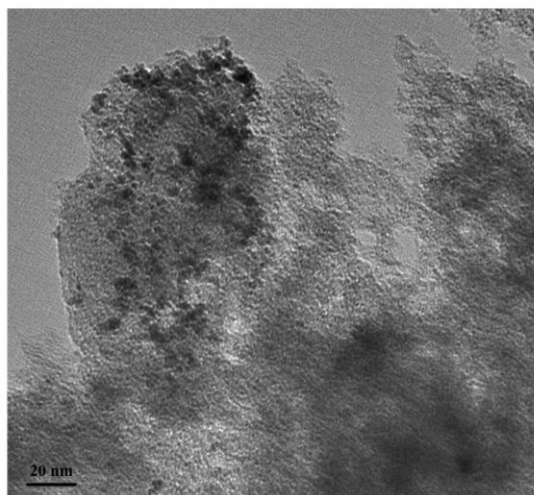
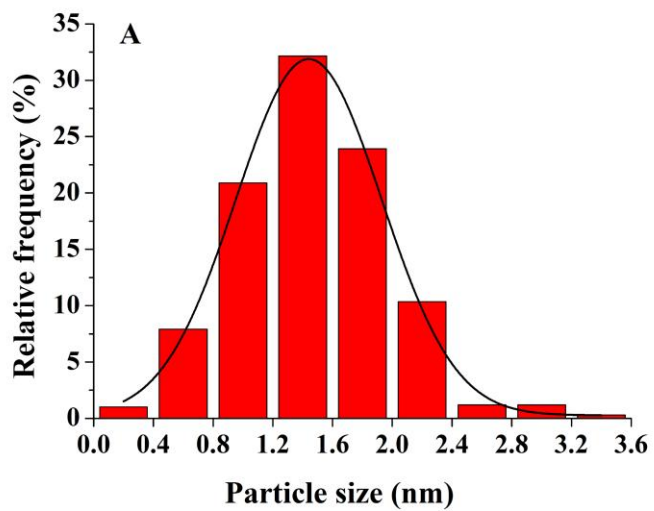
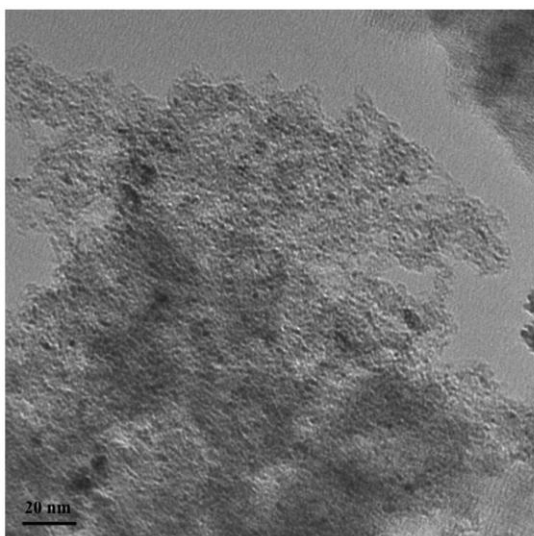
925

926

927

928

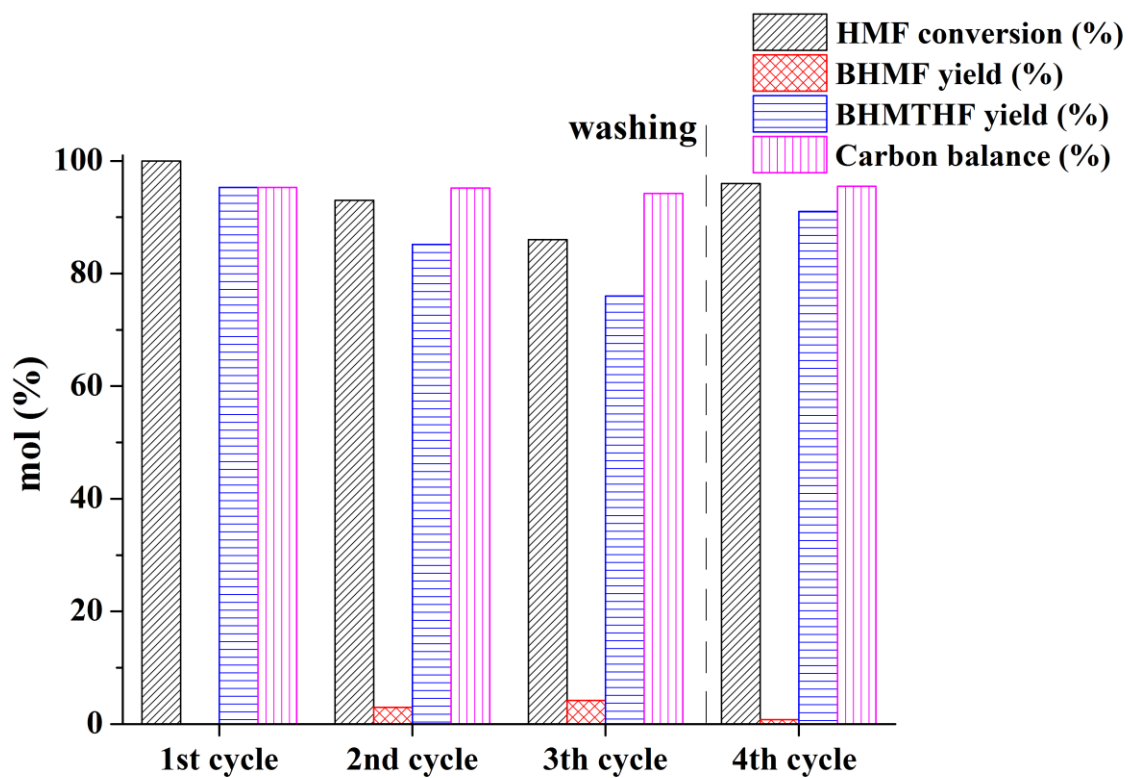
Figure 8



932

Figure 9

933



934

935

936

Supporting Information

Insight into the hydrogenation of pure and crude HMF to furan diols using Ru/C as catalyst

Sara Fulignati^a, Claudia Antonetti^a, Domenico Licursi^a, Matteo Pieraccioni^a, Erwin Wilbers^b, Hero
Jan Heeres^b, Anna Maria Raspolli Galletti^{a,*}

^a Department of Chemistry and Industrial Chemistry, University of Pisa, Via G. Moruzzi 13, 56124,
Pisa, Italy

^b Green Chemical Reaction Engineering, ENTEG, University of Groningen, Nijenborgh 4, 9747 AG
Groningen, The Netherlands

*Corresponding author, e-mail: anna.maria.raspolli.galletti@unipi.it

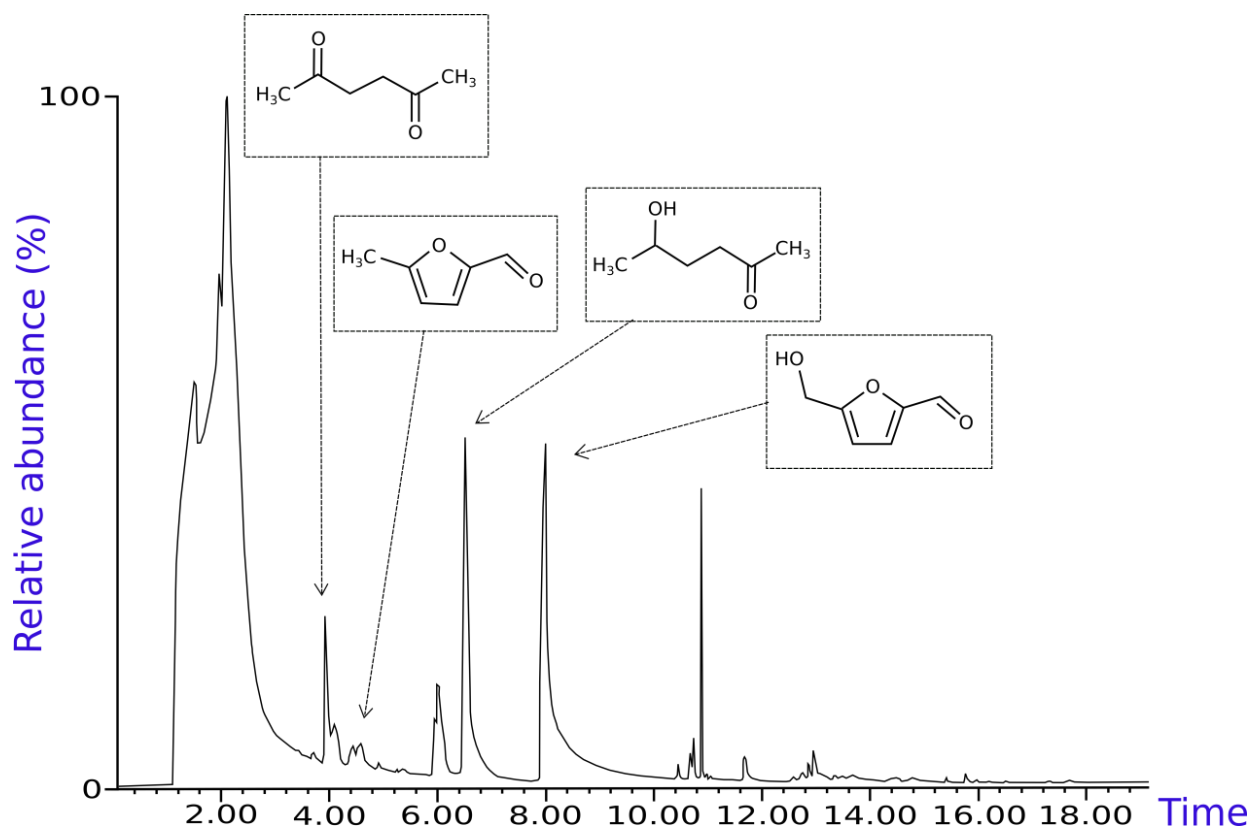


Figure S1 Chromatogram of the final reaction mixture obtained after 1 h working at 140 °C, 70 bar of H₂ in the presence of 5 wt% Pt/C.

15
16
17
18
19
20
21
22
23
24
25
26
27
28
29
30
31
32

33

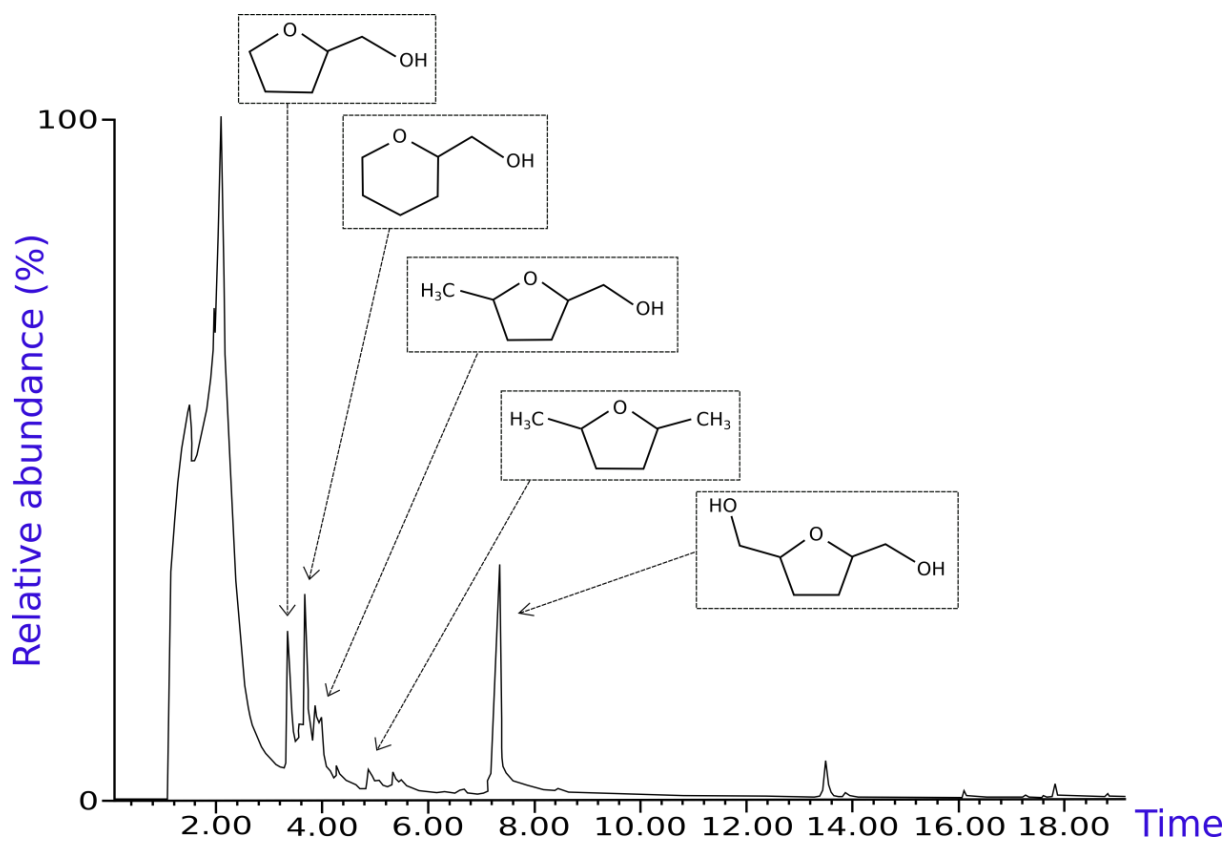
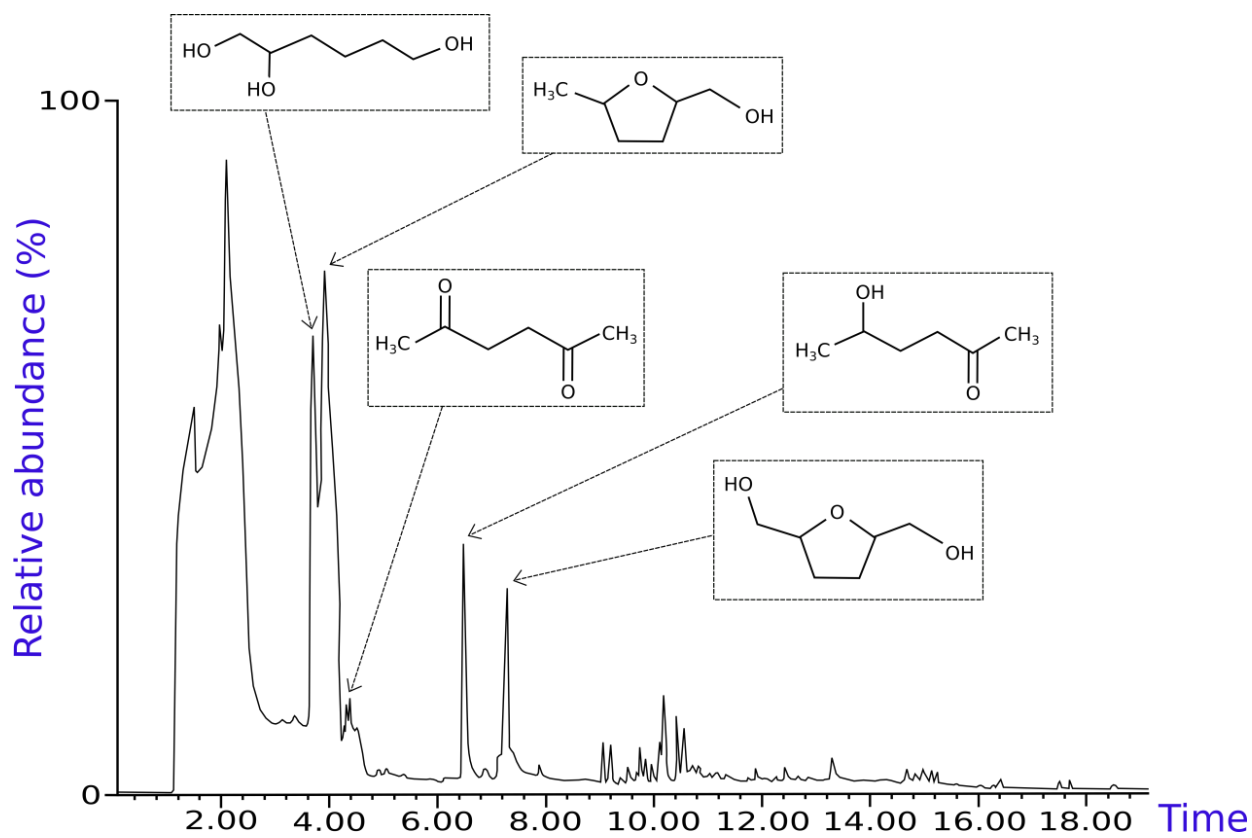


Figure S2 Chromatogram of the final reaction mixture obtained after 1 h working at 140 °C, 70 bar of H₂ in the presence of 5 wt% Ru/C.

51



52

53 **Figure S3** Chromatogram of the final reaction mixture obtained after 1 h working at 140 °C, 70 bar
54 of H₂ in the presence of 5 wt% Pd/C.

55

56

57

58

59

60

61

62

63

64

65

66 **Table S1:** Carbon balance values of the reactions reported in Figure 1. Reaction conditions: [HMF]
67 = 2 wt%; Ru/HMF = 1 wt%; P H₂ = 70 bar.

Run	T (°C)	Carbon Balance (mol%)				
		Time (min)				
		30	60	120	180	240
4	140	79.9	88.9	83.1	82.0	80.1
5	120	92.5	84.9	87.7	92.8	88.0
6	100	94.6	88.0	90.1	93.5	95.0

68

69

70 **Table S2:** Carbon balance values of the reactions reported in Figure 2. Reaction conditions: [HMF]
71 = 3 wt%; Ru/HMF = 1 wt%; P H₂ = 30 bar.

Run	T (°C)	Carbon Balance (mol%)			
		Time (min)			
		30	60	120	240
11	50	100	100	100	99.5
12	70	100	99.0	96.8	67.6
13	100	92.9	72.1	40.4	29.6
14	120	57.4	35.5	29.6	7.4

72

73 **Table S3:** Carbon balance values of the reactions reported in Figures 3, 4, 5 and 7. ^a Reaction
 74 conditions: [HMF] = 3 wt%; Ru/HMF = 1 wt%; T = 100 °C; P H₂= 50 bar. ^b Reaction conditions:
 75 [HMF] = 3 wt%; Ru/HMF = 1 wt%; T = 140 °C; P H₂= 70 bar.

Run	Substrate	Carbon Balance (mol%)			
		Time (min)			
		30	60	120	240
15^a	Hydrolyzate	78.8	66.3	30.2	8.2
16^a	HMF + fructose	97.0	87.5	92.3	95.3
17^a	HMF + formic and levulinic acids	46.5	34.4	7.8	5.6
18^a	HMF + formic acid	53.8	34.4	16.6	10.8
19^a	HMF + levulinic acid	74.6	53.2	22.1	17.1
20^a	Neutralized hydrolyzate	98.0	97.5	80.1	74.5
21^b	Neutralized hydrolyzate	94.2	92.8	80.4	81.0

76

77

78

79

80

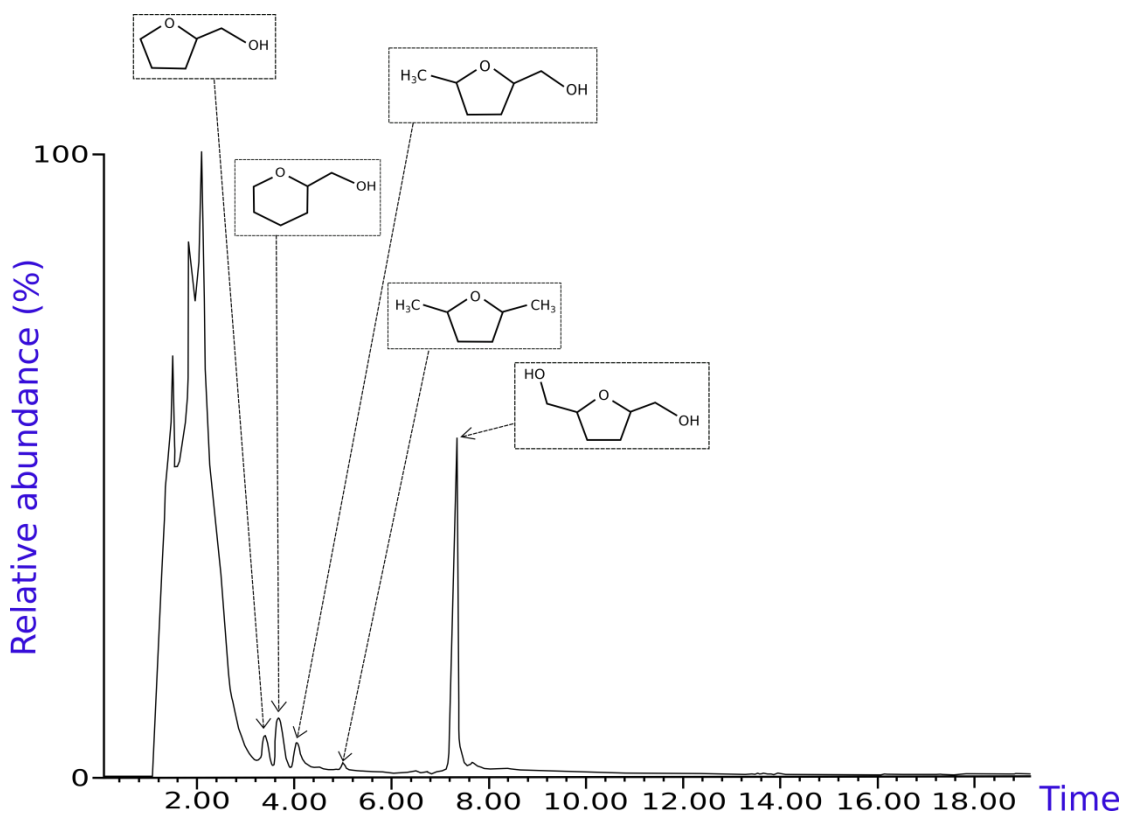
81

82

83

84

85



86

87 **Figure S4** Chromatogram of the final reaction mixture obtained after 4 h working at 100 °C, 50 bar

88 H_2 in the presence of 5 wt% Ru/C.

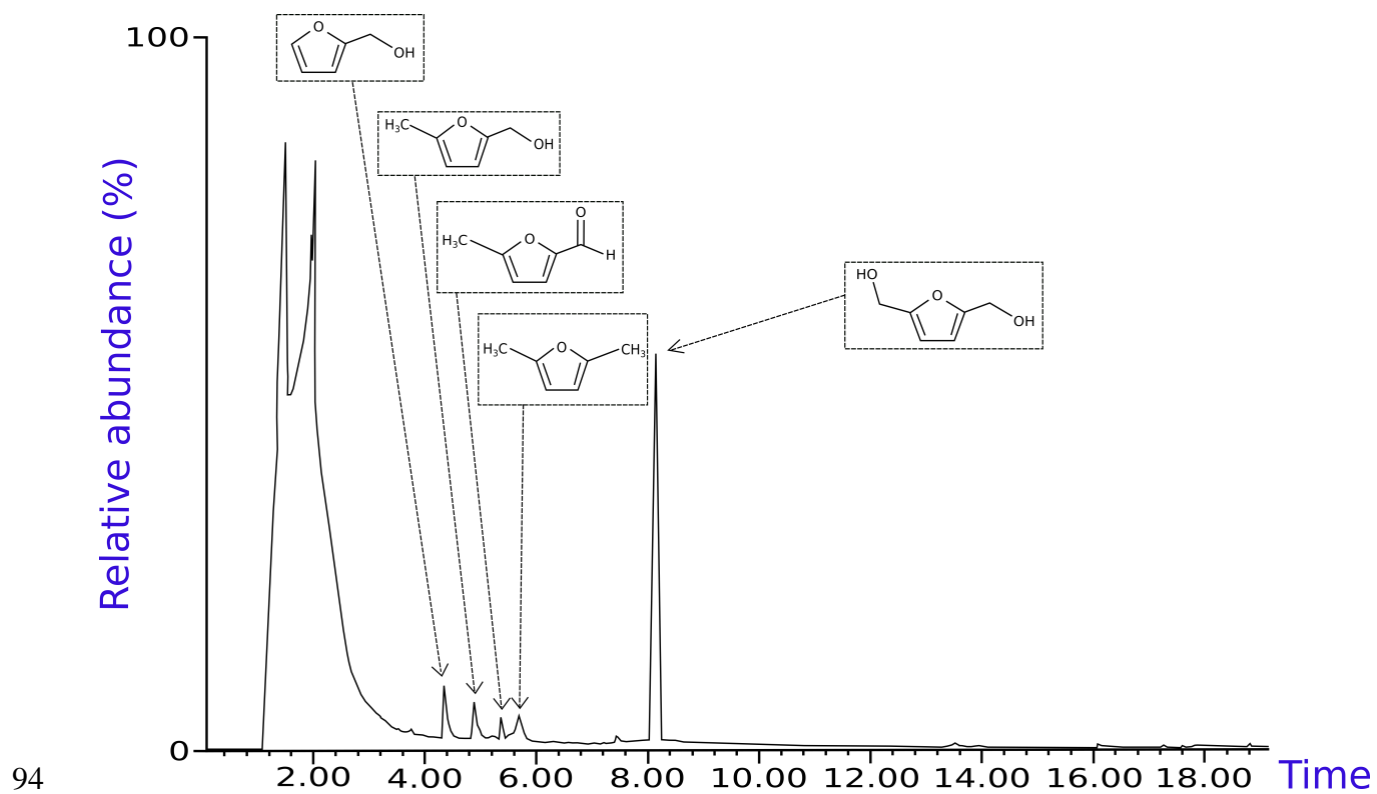
89

90

91

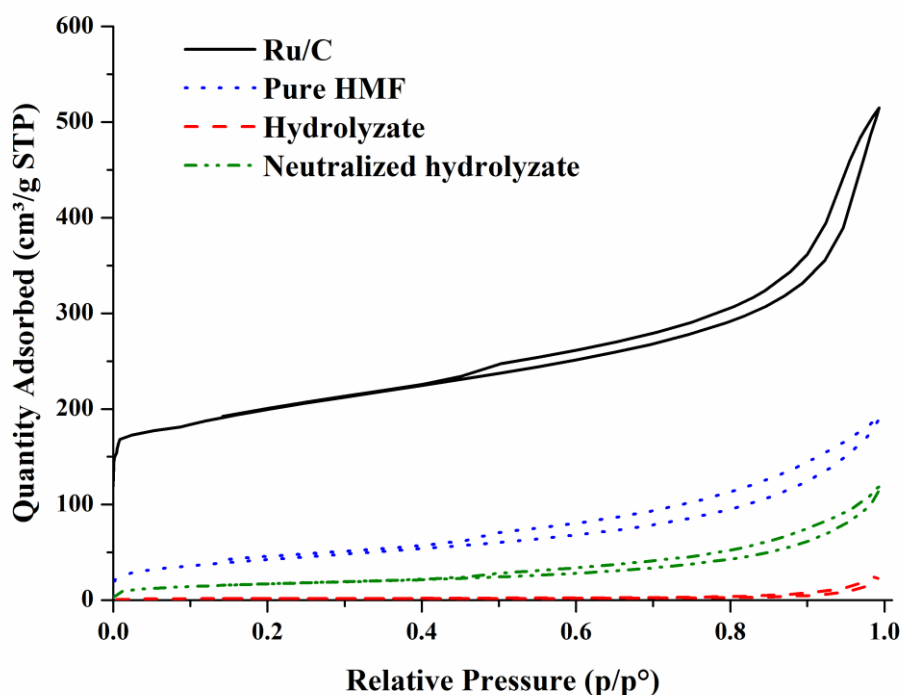
92

93



94
 95 **Figure S5** Chromatogram of the final reaction mixture obtained after 4 h working at 50 °C, 30 bar
 96 H_2 in the presence of 5 wt% Ru/C.

97
 98
 99
 100



101

102 **Figure S6** N₂ physisorption experiment analysis of fresh and spent Ru/C catalysts recovered at the
 103 end of the hydrogenation reactions starting from different initial substrates. Reaction conditions:
 104 [HMF] = 3 wt%; Ru/HMF = 1 wt%; T = 100 °C; P H₂ = 50 bar; t = 240 min.

105

106 **Table S4** Physical properties of fresh and spent Ru/C catalysts at the end of hydrogenation
 107 reactions starting from different initial substrates. Reaction conditions: [HMF] = 3 wt%;
 108 metal/HMF = 1 wt%; T = 100 °C; P H₂ = 50 bar; t = 240 min.

Catalyst (reaction conditions)	Specific surface area (m ² /g)	Total pore volume (cm ³ /g)
Fresh Ru/C	770	0.68
Spent Ru/C (pure HMF)	153	0.26
Spent Ru/C (hydrolyzate)	6	0.02
Spent Ru/C (neutralized hydrolyzate)	62	0.14

109